Copy 6
RM L55E19

NACA RM L55E19

RESEARCH MEMORANDUM

A STUDY OF SERVICE-IMPOSED MANEUVERS OF FOUR JET FIGHTER AIRPLANES IN RELATION TO THEIR HANDLING QUALITIES AND CALCULATED DYNAMIC CHARACTERISTICS

By John P. Mayer and Harold A. Hamer

Langley Aeronautical Laboratory
Langley Field, Va.

NATIONAL ADVISORY COMMITTEE
FOR AERONAUTICS

WASHINGTON

August 15, 1955

NATIONAL ADVISORY COMMITTEE FOR AERONAUTICS

RESEARCH MEMORANDUM

A STUDY OF SERVICE-IMPOSED MANEUVERS OF FOUR JET FIGHTER AIRPLANES IN RELATION TO THEIR HANDLING QUALITIES AND CALCULATED DYNAMIC CHARACTERISTICS

By John P. Mayer and Harold A. Hamer

SUMMARY

Results from a flight program conducted to obtain information on the airplane response and actual rates and amounts of control motion used by service pilots in performance of squadron operational training missions with jet fighter airplanes are correlated with the airplane handling qualities and calculated maximum dynamic response. The correlation indicates that the service pilots in general made use of the static capabilities of their airplanes over most of the speed range as limited either by the control stops or control forces. The maximum responses measured in these service training operations, however, were considerably less than the maximum calculated dynamic response. In longitudinal maneuvers, it is indicated that the pilots have a tendency to maneuver the airplane near its natural frequency.

From the results of the calculations of maximum dynamic response for the North American F-86 airplane, it is indicated that pitching accelerations greater than 16 radians per second per second are theoretically within the range of the pilot and airplane capabilities, whereas the highest value obtained in the tests was about 2 radians per second per second. For lateral maneuvers the calculations indicate that the highest vertical-tail loads for the F-86 airplane could generally be obtained in fishtail maneuvers; however, the calculations indicate that, if rolling pull-out maneuvers were made near the maximum lift coefficient, the vertical-tail loads obtained could be greater than those obtained in fishtail maneuvers. The transverse load factors measured in the present tests were much less than those theoretically obtainable.

INTRODUCTION

In order to obtain information on the airplane response and the amounts and rates of control used by service pilots in operational

training missions, the National Advisory Committee for Aeronautics with the cooperation of the U. S. Air Force and the Bureau of Aeronautics, Navy Department, has conducted a flight program with several jet-propelled fighter airplanes. Information of this type is needed in order to assist in improving design-load criteria.

In reference 1 the results from this program have previously been summarized as envelopes of the maximum values of the measured quantities and the data were compared with design requirements. In addition, a limited statistical analysis was presented. The purpose of this paper is to correlate the results previously obtained in these tests with the airplane stability and handling qualities and compare the maximum values of the measured quantities with the theoretical maximum values obtainable in dynamic maneuvers.

SYMBOLS

b	wing span, ft
c	wing mean aerodynamic chord, ft
$C_1, C_2, C_3, \ldots$	constants appearing in lateral equations of motion
C_{l_β}	rate of change of airplane rolling-moment coefficient with angle of sideslip, $\partial C_l/\partial\beta$, per radian
C_{l_p}	rate of change of airplane rolling-moment coefficient with $\dot{\phi}b/2V$, per radian
C_{l_r}	rate of change of airplane rolling-moment coefficient with $\dot{\psi}b/2V$, per radian
$C_{l_{\delta_A}}$	rate of change of airplane rolling-moment coefficient with total aileron deflection, $\partial C_l/\partial\delta_A$, per radian
C_{n_β}	rate of change of airplane yawing-moment coefficient with angle of sideslip, $\partial C_n/\partial\beta$, per radian
C_{n_p}	rate of change of airplane yawing-moment coefficient with $\dot{\phi}b/2V$, per radian
C_{n_r}	rate of change of airplane yawing-moment coefficient with $\dot{\psi}b/2V$, per radian
$C_{n_{\delta_A}}$	rate of change of airplane yawing-moment coefficient with total aileron deflection, $\partial C_n/\partial\delta_A$, per radian

C_{Y_β}	rate of change of airplane lateral-force coefficient with angle of sideslip, $\partial C_Y/\partial\beta$, per radian
C_{m_o}	zero-lift wing-fuselage pitching-moment coefficient
$C_{m_{WF}}$	wing-fuselage pitching-moment coefficient
$C_{N_{WF}}$	wing-fuselage normal-force coefficient
d	distance from airplane center of gravity to aerodynamic center of wing-fuselage combination, ft
F_E	elevator stick force, lb
g	acceleration due to gravity, 32.2 ft/sec^2
I_X	airplane moment of inertia about longitudinal axis, slug-ft^2
I_Y	airplane moment of inertia about lateral axis, slug-ft^2
I_Z	airplane moment of inertia about vertical axis, slug-ft^2
I_{XZ}	airplane product of inertia, slug-ft^2
$K_1, K_2, K_3, \ldots$	dimensional constants appearing in longitudinal equations of motion
L_T	horizontal-tail load, lb
m	airplane mass, W/g, slugs
n	normal load factor
n_o	initial value of normal load factor (used in rolling pull-out solution)
n_T	transverse or lateral load factor
q	dynamic pressure, 1/2 ρV^2, lb/ft^2
q_c	impact pressure, lb/ft^2
S	total wing area, ft^2

t	time, sec
T_{90}	time to roll 90°, sec
V	true airspeed, ft/sec
V_i	indicated airspeed, knots
W	airplane gross weight, lb
x_t	distance from airplane center of gravity to aerodynamic center of horizontal tail, ft
β	airplane angle of sideslip (defined herein as angle between longitudinal axis and projection of relative wind in horizontal plane of airplane), radians (except when noted otherwise)
β_{eff}	effective angle of sideslip used in fishtail and rolling pull-out calculations
$\dot{\beta}$	time rate of change of angle of sideslip, radians/sec
Δ	increment
δ_A	aileron deflection (total, except when noted otherwise), radians (except when noted otherwise)
δ_E	elevator deflection, radians (except when noted otherwise)
$\delta_{E_{max}}$	maximum calculated elevator deflection, radians
$\delta_{E_{lim}}$	elevator deflection limit, radians (except when noted otherwise)
$\dot{\delta}_E$	elevator deflection rate, radians/sec
$\dot{\delta}_{E_{max}}$	maximum calculated elevator deflection rate, radians/sec
$\dot{\delta}_{E_{lim}}$	elevator deflection rate limit, radians/sec
δ_R	rudder deflection, radians (except when noted otherwise)
$\dot{\theta}$	pitching angular velocity, radians/sec

$\dot{\theta}_o$	initial value of pitching angular velocity (used in rolling pull-out solution), radians/sec
$\dot{\theta}_{max}$	maximum calculated pitching angular velocity, radians/sec
$\ddot{\theta}$	pitching angular acceleration, radians/sec^2
$\ddot{\theta}_{max}$	maximum calculated pitching angular acceleration, radians/sec^2
ρ	mass density of air, slug/ft^3
ϕ	angle of bank, radians
$\dot{\phi}$	rolling angular velocity, radians/sec
$\ddot{\phi}$	rolling angular acceleration, radians/sec^2
$\phi_{\ddot{\theta}_n}$	phase angle between pitching angular acceleration and incremental normal load factor, deg
$\dot{\psi}$	yawing angular velocity, radians/sec
$\ddot{\psi}$	yawing angular acceleration, radians/sec^2
ω	angular frequency, radians/sec
ω_n	natural angular frequency, radians/sec

A bar over symbol represents maximum value and | | represents absolute value.

AIRPLANES

The airplanes for which measurements were available were service models of the North American F-86A, McDonnell F2H-2, Republic F-84G, and Lockheed F-94B. All were low-wing jet-propelled fighter-type airplanes, the F-86A having a swept wing and empennage. All were equipped with hydraulic aileron boost. In addition, the elevator for the F-86A was hydraulically boosted and was equipped with an adjustable stabilizer. A rate restrictor is also incorporated in the F-86A elevator control system and restricted the elevator rate to about 45° per second.

In the tests, the F-86A and F-94B airplanes were flown, for the most part, without external fuel tanks and the F2H-2 and F-84G airplanes were flown, for the most part, with external fuel tanks.

Except for the addition of sideslip and angle-of-attack booms neither the external appearance nor the weight and balance of the airplanes was altered by the addition of the NACA instrumentation. Three-view drawings of the airplanes are presented in figure 1. Dimensions and physical characteristics of the airplanes are given in table 1.

INSTRUMENTATION AND TESTS

The airplanes used during the flight program were fully instrumented with standard NACA photographically recording instruments which measured (1) the quantities defining the flight conditions, such as airspeed and altitude, (2) the imposed control-surface motions, and (3) the response of the airplane in terms of load factors, angular velocities, angular accelerations, and angle of sideslip.

The maximum errors estimated for the measured quantities given in this paper are as follows:

Control-surface angle, deg	±0.7
Normal load factor	±0.1
Transverse load factor	±0.03
Pitching angular velocity, radian/sec	±0.03
Rolling angular velocity, radian/sec	±0.15
Yawing angular velocity, radian/sec	±0.02
Pitching angular acceleration, radian/sec^2	±0.1
Angle of sideslip, deg	±0.7

More complete details of the instrumentation are given in reference 1.

All flights obtained during the program were performed by service pilots undergoing regular squadron operational training. Data were recorded continuously throughout a flight and were recorded only during those flights in which the mission was scheduled to include a large number of maneuvers. The primary missions were usually acrobatics, ground gunnery, aerial gunnery, or dive-bombing and the maneuvers recorded during the program included most of the tactical maneuvers that were within the capabilities of the individual airplanes. These maneuvers were performed at altitudes up to approximately 35,000 feet and at airspeeds varying from the stalling airspeed to the maximum service limit airspeed. Most of the maneuvers were performed in relatively smooth air. No attempt was made to specify the type or severity of maneuvers.

During the test program a total flight time of about 60 hours was recorded. However, since the pilots were requested to perform as many

maneuvers as practical during each flight the data are believed to be representative of many more hours than were actually recorded.

A total of 42 service pilots participated with no one pilot accounting for more than 20 percent of the maneuver time obtained for the particular make airplane. Although the pilots were aware of the instrumentation, it was stressed that this was not to restrict their normal handling of the airplane since they would not be personally identified with the test results.

ORGANIZATION OF DATA AND METHODS OF ANALYSIS

In the presentation of the data the results are presented in three groups: (1) longitudinal characteristics, (2) rolling characteristics, and (3) sideslip characteristics. For these three groups the envelopes of the various quantities obtained in these tests for each airplane are compared with the airplane stability and control characteristics. Also, for the longitudinal and sideslip groups, the test envelopes are compared with the maximum values theoretically possible under dynamic conditions. In the longitudinal case, calculations are made only for the F-86A airplane and are compared with overall envelopes representing boundaries for all the test airplanes. In the sideslip group, the calculations are made, for the most part, for the F-86A and F-84 airplanes and are compared with the test envelopes of the individual airplanes. The calculations for the F-84 airplane are based on earlier models (A through D) which had a fuselage that was 18 inches shorter than that of the test airplane.

In the data plots, only those maximum values which helped to establish the envelopes are shown. In general, the test boundaries are established by considering only those maneuvers where controlled flight is maintained. The envelopes of the data representing other flight conditions such as low-speed stalls, snap rolls, and lateral oscillations are also shown, superimposed on the main test boundary. Further discussion regarding the basic data and the construction of the envelopes, both for the individual airplanes and the combination representing all the test airplanes, may be found in reference 1.

RESULTS AND DISCUSSION

The results presented in this paper for the F-86A, F2H-2, F-84G, and the F-94B airplanes are compared with the results of tests presented in references 2 to 8. In some cases the airplanes from these references are not the same models as those used in the present flight

program. However, the dimensions and physical characteristics for each type airplane are the same, except for minor differences in some of the airplanes regarding external-fuel-tank location.

Since many of the quantities to be discussed are related to and limited by the airplane V-n diagram, the maximum positive and negative normal load factors and corresponding indicated airspeeds reached with each airplane were taken from reference 1 and are presented as figure 2 in this paper.

Longitudinal Characteristics

Elevator position and force.- The envelopes of maximum elevator angles obtained are shown in figure 3. Also shown in figure 3 are the elevator angles necessary to reach the V-n envelope in gradual maneuvers as derived from references 2, 5, 7, and 8. For the F-86A airplane values are shown for stabilizer angles of 0° and 2°, airplane nose up, which correspond to the minimum and average trim stabilizer angles used in these tests, respectively. It may be noted from figure 3 that the elevator angles used equaled or exceeded the static values necessary to reach the limits of the V-n diagram in the regions where these limits (see fig. 2) were reached in the operational maneuvers. The angles shown above the static curve were associated with more rapid maneuvers such as abrupt pull-outs, turns, and rolls where a larger elevator angle was used than was necessary to reach a given steady value of load factor.

Since stick forces were not measured in the present tests the forces were derived from stick force data of references 3, 5, 7, and 8 and are presented in figure 4. In figure 4 the maximum elevator stick forces necessary to reach the V-n envelope at low altitudes are compared with the minimum and maximum force requirements of references 9 and 10. The stick forces for all the test airplanes were within the maximum and minimum stick force requirements except for the F-84G airplane where the elevator forces would appear to be higher than the maximum forces specified by the requirements. The stick forces required for the F-86A airplane to reach the V-n envelope appear to be within the limits given by the requirements; however, the curve shown does not indicate the stick force reversal which occurs at the pitch up. At high altitudes the stick forces at the limits of the V-n diagram are very low because of this force reversal. In the present tests the test airplane did encounter pitch up but at altitudes less than 15,000 feet. The elevator stick forces for the F2H-2 and F-94B airplanes are near the minimum requirement at high speeds.

Pitching acceleration.- Pitching angular acceleration is one of the important parameters in the determination of horizontal-tail loads.

If the rolling and yawing motions of the airplane are small, the horizontal-tail load in any maneuver could be given by

$$L_T = C_{m_o} qS \frac{c}{x_t} + nW \frac{d}{x_t} - \frac{I_y}{x_t} \ddot{\theta} \tag{1}$$

or

$$L_T = C_{m_o} qS \frac{c}{x_t} + nW \frac{c}{x_t} \frac{C_{m_{WF}}}{C_{N_{WF}}} - \frac{I_y}{x_t} \ddot{\theta} \tag{2}$$

Thus, if the maximum pitching accelerations could be predicted, the maximum incremental horizontal-tail loads could be calculated. In reference 1 the maximum pitching accelerations obtained in operational training are compared with several design methods or requirements. This plot taken from reference 1 is shown in figure 5 as a matter of interest. The curves for the design methods or requirements shown in figure 5 are either empirical or based on performing a single abrupt maneuver to the limit load factor from 1 g flight. (Refs. 1 and 11 to 15.)

In order to show the theoretical maximum pitching acceleration obtainable in flight, calculations were made for the F-86 airplane in which the airplane was maneuvered sinusoidally to the load-factor limits. In these computations the equation of motion was expressed as in reference 16.

$$\ddot{n} + K_1\dot{n} + K_2\Delta n = K_7\Delta\delta_E + K_8\dot{\delta}_E + K_9\ddot{\delta}_E \tag{3}$$

and in terms of θ as

$$\ddot{\theta} + K_1\dot{\theta} + K_2\Delta\theta = K_5\Delta\delta_E + K_6\int_0^t \Delta\delta_E dt \tag{4}$$

The amplitude ratio $\left|\overline{\Delta n}/\overline{\Delta\delta_E}\right|$ for a sinusoidal-control motion may be shown to be

$$\left|\frac{\overline{\Delta n}}{\overline{\Delta\delta_E}}\right| = \sqrt{\frac{K_8{}^2\omega^2 + \left(K_7 - K_9\omega^2\right)^2}{\left(K_2 - \omega^2\right)^2 + K_1{}^2\omega^2}} \tag{5}$$

The amplitude ratio $\left|\overline{\dot{\theta}}/\overline{\Delta\delta_E}\right|$ is

$$\left|\frac{\overline{\dot{\theta}}}{\overline{\Delta\delta_E}}\right| = \sqrt{\frac{K_6^2 + K_5^2\omega^2}{\left(K_2 - \omega^2\right)^2 + K_1^2\omega^2}} \tag{6}$$

and the amplitude ratio $\left|\overline{\ddot{\theta}}/\overline{\Delta\delta_E}\right|$ is

$$\left|\frac{\overline{\ddot{\theta}}}{\overline{\Delta\delta_E}}\right| = \sqrt{\frac{\omega^2\left(K_6^2 + K_5^2\omega^2\right)}{\left(K_2 - \omega^2\right)^2 + K_1^2\omega^2}} \tag{7}$$

The phase angle between $\ddot{\theta}$ and n is then

$$\phi_{\ddot{\theta}_n} = \tan^{-1}\frac{K_6}{K_5\omega} - \tan^{-1}\frac{K_8\omega}{K_7 - K_9\omega^2} \tag{8}$$

The stability derivatives for the K constants required in the above equations were obtained from wind-tunnel tests. (See refs. 17 and 18.)

Typical frequency-response curves calculated for the F-86 airplane are shown in figure 6 for a speed of 300 knots at sea level. The absolute values for the amplitude ratios $\left|\overline{\Delta n}/\overline{\Delta\delta_E}\right|$, $\left|\overline{\dot{\theta}}/\overline{\delta_E}\right|$, and $\left|\overline{\ddot{\theta}}/\overline{\delta_E}\right|$ are shown as well as the phase angle between $\ddot{\theta}$ and n.

In figure 7 calculated values of the elevator angle, maximum elevator rate, maximum pitching velocity, and maximum pitching acceleration are shown plotted against angular frequency. These values were obtained from the frequency-response curves given in figure 6 for a sinusoidal maneuver from a load factor of -3 to a load factor of 7.33 at an airspeed of 300 knots at sea level. It can be seen that the maximum pitching acceleration increases throughout the frequency range shown and would finally be limited either by the amount of elevator available or by the highest elevator rate obtainable. The largest elevator angle available was 0.458 radian (26.25°) and the highest elevator rate was assumed to be 3.5 radians per second (200° per second). Also indicated in figure 7 is the maximum pitching acceleration for an elevator rate of 0.785 radian per second (45° per second) which corresponds to the maximum elevator rate obtainable with F-86A airplanes equipped with elevator rate restrictors.

Calculations similar to those of figures 6 and 7 were made for the F-86A airplane for several additional airspeeds at sea level and for an airspeed of 400 knots at 20,000 feet. The results are shown plotted against airspeed in figures 8 to 10 along with the results obtained in the test program with operational airplanes.

In figure 8 the maximum calculated pitching acceleration is shown for two cases. In the first case the airplane is maneuvered sinusoidally from its negative load-factor limits to its positive load-factor limits as defined by the V-n diagram. (See fig. 2.) At low speeds the maximum load factors are associated with maximum lift and at high speeds the maximum load factors are the design limit load factors (-3 and 7.33). In the second case the airplane is maneuvered sinusoidally from the 1 g level-flight condition to its positive maximum load-factor limits. The maximum pitching accelerations shown for the two cases are limited by reaching the elevator deflection limit (0.458 radian) or by reaching the highest possible elevator rates (3.5 radians per second or 0.785 radian per second).

It may be seen in figure 8 that maximum pitching accelerations as high as 16 radians per second per second are theoretically possible and, as indicated in figure 6, the maximum negative pitching acceleration would be approximately in phase with the maximum positive normal load factor (and vice versa). This condition results in maximum horizontal-tail loads in subsonic flight. It may be noted that the points shown for an altitude of 20,000 feet are approximately the same as those for sea-level conditions when plotted against indicated airspeed.

In figure 9 maximum pitching accelerations are shown for a sinusoidal maneuver at two constant angular frequencies and at the natural frequency of the airplane. Also shown is the test boundary from the present tests. Pitching accelerations are shown for angular frequencies of 6.28 and 3.14 radians per second which correspond to a time to reach maximum load factor of 0.5 second and 1 second, respectively, and for the undamped natural frequency of the airplane $\omega = \sqrt{K_2}$.

It can be seen in figure 9 that the maximum pitching acceleration at a constant angular frequency decreases with airspeed at the higher speeds whereas the maximum pitching acceleration at the airplane natural frequency is proportional to the load factor and remains about the same at speeds above that of the upper left-hand corner of the V-n diagram. It is of interest to note that the maximum pitching accelerations obtained in the present tests of service airplanes are approximately the same as those calculated at the airplane undamped natural frequency at speeds up to 350 knots. This result would tend to confirm the belief that pilots have a tendency to maneuver the airplane near its natural frequency. At the higher speeds the natural frequency is higher and therefore the time to reach maximum load factor would be less than at low speeds. The lower values of the experimental pitching accelerations at the higher speeds are probably due to the hesitancy of pilots to perform rapid high load-factor maneuvers at high speeds.

The variation of maximum pitching acceleration in maneuvering from 1 g to the positive load-factor limits is shown in figure 10. Values are

shown for the case of figure 8 where the pitching acceleration is limited either by reaching the elevator limits or by reaching a limiting elevator rate, for the case of figure 9 where the pitching acceleration is shown for a constant angular frequency, and for the case where the airplane is maneuvered at its natural frequency. Also shown are the maximum pitching accelerations calculated by the method of reference 11 in which the airplane is maneuvered from 1 g to its positive load-factor limits with a minimum time to reach the maximum load factor of about 0.5 second as well as the maximum pitching accelerations measured in the service training operations.

In figure 10 it is noted that the maximum pitching accelerations calculated by maneuvering the airplane sinusoidally at a constant angular frequency of 6.28 radians per second are approximately the same as those of the method of reference 11. In both cases the time to reach maximum load factor is about 0.5 second. The maximum pitching acceleration that could be reached with the limit elevator rate, however, is almost three times as high as that calculated for a very abrupt maneuver or with an angular frequency of 6.28 radians per second. The maximum pitching accelerations measured in the present test program and the pitching accelerations calculated at the airplane natural frequency are less than one half the values that could be obtained in an abrupt maneuver or a pitching oscillation at $\omega = 6.28$ radians per second.

It is evident that values of the pitching acceleration as high as 16 radians per second per second calculated by using the limiting characteristics of the pilot and airplane are probably unreasonable to use in tail-load design since the maneuvers necessary to produce such accelerations would be of negligible order of probability. On the other hand, the maximum pitching accelerations of from 5 to 6 radians per second per second shown in figure 10 obtained by the method of reference 11 or by using a constant value of the angular frequency $\omega = 6.28$ are values that could be reached if the pilots maneuvered the airplane in the manner specified. Pitching accelerations of this order have been obtained in research and structural integrity flight tests of fighter airplanes. In the present limited tests of jet fighter airplanes, it is indicated that the pilots tend to maneuver their airplanes near the airplane natural frequency which involves maximum pitching accelerations of less than three radians per second per second.

Pitching angular velocity.- In figure 11 the maximum calculated pitching velocities are compared with the experimental values obtained in service training operations. The maximum calculated pitching velocities were obtained in a pitching oscillation from the negative load-factor limit to the positive load-factor limit and from 1 g to the positive load-factor limit by using the limiting elevator angles or rates. Also shown are the values for maximum pitching velocities calculated for a constant angular frequency of 6.28 radians per second,

the values calculated for the airplane natural frequency, and the values calculated by the method of reference 11 for a time to reach a peak load factor of about 0.5 second.

It may be seen that pitching velocities as high as 1.6 radians per second may be obtained within the limitations of the pilot and airplane. In abrupt pull-ups and at a constant pitching angular frequency of 6.28 radians per second, pitching velocities of about 1 radian per second are possible. Except in stalls, the highest pitching velocity measured in the present tests was about 0.5 radian per second. As was the case for pitching acceleration the pitching velocities calculated at the airplane natural frequency are near the experimental values except at the higher speeds.

Rolling Characteristics

Aileron angles.- The maximum aileron angles obtained in the service operational training are shown in figure 12 as well as the maximum angles available as derived from references 4, 6, 7, and 8. The maximum available aileron angle shown is, for low speeds, the full aileron deflection and, for higher speeds, the aileron deflection as limited by 30 pounds stick force or maximum boost. The F-84G airplane was the only airplane to use full aileron and these points were mostly obtained in stalls at low speeds. The F-86, the F-84, and the F-94 aileron angles used appeared to be limited by aileron forces or boost limitations at high speeds. The aileron angles used with the F2H airplane reached the limits only in a narrow speed range near 350 knots.

$\dot{\phi}b/2V$.- The maximum values of the helix angle $\dot{\phi}b/2V$ obtained in the present tests are shown in figure 13 along with the maximum values obtainable in abrupt aileron rolls from level flight (refs. 4, 6, 7, and 8). The values of $\dot{\phi}b/2V$ shown correspond to the aileron angles given in figure 12. At the highest speeds all the test airplanes, with the exception of the F2H airplane, reached or approached the maximum values obtainable in abrupt aileron rolls. The F2H airplane did not approach its rolling capabilities except in a small speed range near 350 knots. The F-86 airplane did not make use of its full rolling capabilities at speeds below 300 knots whereas the F-84 and F-94 airplanes approached or reached their rolling capabilities at all speeds. Very high values of $\dot{\phi}b/2V$ were measured with the F-84 airplane in uncontrolled maneuvers (snap rolls and stalls) which exceeded the values that would be obtained in abrupt aileron rolls from level flight.

It can be seen in figure 13 that all the test airplanes used maximum values of $\dot{\phi}b/2V$ up to 0.07 or 0.08 at speeds less than 300 knots even though higher values could have been reached for the F-86 and F2H airplanes.

Rolling velocity.- The maximum rolling velocities measured in the operational training program are shown in figure 14 in addition to the maximum rolling velocities obtainable in aileron rolls from level flight at sea level and at an altitude of 30,000 feet. The experimental values shown were obtained under accelerated flight as well as level-flight conditions. The maximum rolling velocities reached were from about 2.0 to 2.4 radians per second in controlled flight except for the F2H airplane where maximum rolling velocities of about 1.7 radians per second were reached. In uncontrolled flight rolling velocities up to 3.5 radians per second were obtained with the F-84G airplane. It may be noted that the experimental data approximate the shapes of the maximum curves fairly well with the exception of the F2H airplane at high speeds.

Time to roll 90°.- In figure 15 the minimum times to roll 90° in the present tests with service airplanes are compared with the minimum times to roll 90° for each of the airplanes calculated with a hypothetical rolling maneuver where the rolling velocity was a step function. The step rolling velocities used are those labeled limit in figure 14. For the F-94 airplane the curve for 30,000 feet is also shown, and for the F-84 airplane curves are shown for wing-tip tanks on and off. The minimum time required to roll 90° varied from 1 to 1.5 seconds for the test airplanes whereas the absolute minimum varies from about 0.6 to 1.0 second for sea-level conditions.

Sideslip Characteristics

Rudder angle.- The maximum rudder angles measured in the tests during service operational training are shown in figure 16 as well as the limit rudder angle and the rudder angle for 180 pounds pedal force as derived from references 4, 6, 7, and 8. The rudder angles used were less than the maximum available rudder angles except in stalled maneuvers where the limits were approached or reached with F-86 and F-84 airplanes; however, at airspeeds above 250 knots it is indicated that the rudder angles used were limited by high pedal forces for the test airplanes.

Sideslip angle.- The maximum sideslip angles measured are shown in figure 17 in addition to the sideslip angles obtainable in steady sideslips as limited either by reaching the rudder-angle limits or 180 pounds pedal force. Above an airspeed of about 250 knots, the sideslip angles reached or exceeded the sideslip angles for 180 pound pedal force for all the test airplanes. Most of these large sideslip angles were obtained in rolling maneuvers. At the lower speeds the sideslip angles reached with the test airplanes did not approach these limits except for the F-84G airplane in stalls. (It should be noted that, as indicated in reference 1, sideslip angles were not measured in all the flights with the F-86A airplane.)

Comparison of maximum measured sideslip characteristics with maximum theoretical values.- The maximum measured sideslip characteristics are compared with maximum calculated values obtainable in fishtail and rolling pull-out maneuvers in figures 18 to 27. The maximum calculated peak values of the amplitude ratios $\left|\overline{\beta}/\overline{\delta}_R\right|$ and $\left|\overline{\dot{\psi}}/\overline{\delta}_R\right|$ for the F-86A and F-84 airplanes in level-flight fishtail maneuvers were obtained directly from reference 19 and are determined for the frequency response to a sinusoidal rudder input at altitudes of 1,000 and 20,000 feet. The maximum values of β and $\dot{\psi}$ were obtained for the maximum rudder angles as limited by the rudder-angle limits or by reaching 180 pounds rudder pedal force. (See fig. 16.) Values of maximum $\ddot{\psi}$ were then calculated from the expression

$$\left|\frac{\overline{\ddot{\psi}}}{\overline{\delta}_R}\right| = \omega\left|\frac{\overline{\dot{\psi}}}{\overline{\delta}_R}\right| \tag{9}$$

For the rolling pull-out maneuvers, calculations were made only for the F-86A airplane at an altitude of 1,000 feet and 20,000 feet. As in reference 20, the calculations were based on the three nonlinear lateral equations of motion:

$$I_X\ddot{\phi} - I_{XZ}\ddot{\psi} - \left(I_Y - I_Z\right)\dot{\theta}\dot{\psi} - \left(C_{l_\beta}\beta + C_{l_p}\frac{\dot{\phi}b}{2V} + C_{l_r}\frac{\dot{\psi}b}{2V}\right)qSb = C_{l_{\delta_A}}\delta_A qSb \tag{10}$$

$$I_Z\ddot{\psi} - I_{XZ}\ddot{\phi} - \left(I_X - I_Y\right)\dot{\theta}\dot{\phi} - \left(C_{n_\beta}\beta + C_{n_p}\frac{\dot{\phi}b}{2V} + C_{n_r}\frac{\dot{\psi}b}{2V}\right)qSb = C_{n_{\delta_A}}\delta_A qSb \tag{11}$$

$$mV(\dot{\beta} + \dot{\psi}) - W\phi - C_{Y_\beta}\beta qS = 0 \tag{12}$$

These equations were linearized by assuming that the pitching velocity was constant and equal to

$$\dot{\theta}_o = \frac{(n_o - 1)g}{V} \tag{13}$$

The cross-coupled inertia terms were then included as additions to C_{l_r} and C_{n_p} in equations (10) and (11). Solutions were obtained over the

speed range by using the Reeves Electric Analog Computer (REAC) for rolling pull-outs at the maximum load factor as given by the V-n diagram of figure 2. A step aileron input was used which was equal to the maximum aileron angle as limited either by full throw or by 30 pounds stick force. (See fig. 12.) It was assumed that the rudder was held fixed and that the pitching velocity was constant. The maximum values of the parameters shown are given at the first peak in the oscillation because subsequent peaks usually were unreliable since the angles involved exceeded the range for which equations (10) to (12) are valid. The derivatives used in equations (10) to (12) were obtained from references 19 and 21.

Maximum calculated values of n_T obtainable in fishtail maneuvers for the F-86A and F-84 airplanes were obtained by determining the ratio $\left|\overline{n_T}/\overline{\delta_R}\right|$ to $\left|\overline{\beta}/\overline{\delta_R}\right|$ at the natural frequency, which is approximately

$$\omega_n = \sqrt{C_{n_\beta} \frac{qSb}{I_Z}} \tag{14}$$

The amplitude ratios may be expressed as

$$\left|\frac{\overline{\beta}}{\overline{\delta_R}}\right| = \sqrt{\frac{\left(C_8 - C_6\omega^2\right)^2 + \left(C_7 - C_5\omega^3\right)^2}{\left(\omega^4 - C_2\omega^2 + C_4\right)^2 + \left(C_3\omega - C_1\omega^3\right)^2}} \tag{15}$$

and

$$\left|\frac{\overline{n_T}}{\overline{\delta_R}}\right| = \frac{1}{g}\sqrt{\frac{\left(C_{16}\omega^4 - C_{18}\omega^2 + C_{20}\right)^2 + \left(C_{19}\omega - C_{17}\omega^3\right)^2}{\left(\omega^4 - C_2\omega^2 + C_4\right)^2 + \left(C_3\omega - C_1\omega^3\right)^2}} \tag{16}$$

Maximum values of n_T obtainable in rolling pull-out maneuvers for the F-86A airplane were obtained by using the approximate relationship:

$$n_T = \frac{C_{Y_\beta}\beta q}{W/S} \tag{17}$$

The constants in equations (15) and (16) are defined as in reference 22. In solving these equations, values for the derivatives were obtained from references 19 and 21.

Sideslip angle: The test boundaries along with the calculated values of sideslip angle in fishtails are shown in figures 18 and 19 for the F-86A and F-84G airplanes, respectively. Calculated values of sideslip angle in rolling pull-outs are also shown for the F-86A in figure 18. The angles of sideslip obtainable in fishtails appear to be about 3 to 4 times as great as those reached with the service airplanes. For the F-86 airplane it can be seen in figure 18 that the sideslip angles obtainable in rolling pull-outs are lower than those obtainable in fishtails above an airspeed of 330 knots. Below this speed the maximum angles of sideslip calculated in rolling pull-outs increased rapidly and were greater than those obtainable in fishtail maneuvers. The values of the maximum sideslip angle obtainable in rolling pull-outs are not shown at lower speeds since the angles of sideslip and roll obtained from the calculations were much larger than those for which equations (10) to (12) are valid. The results indicated, however, that the maximum sideslip angle in rolling pull-outs increased with airspeed and reached a peak at about 300 knots and then decreased abruptly as shown in figure 18.

βq and transverse load factor: In figures 20 and 21 are shown the values of the parameter βq for the F-86A and F-84G airplanes and in figures 22 and 23 the transverse load factors for the two airplanes are shown. The parameter βq is given since it is roughly proportional to the vertical-tail load. For sideslip angles greater than 10°, the parameter βq is based on an effective value of β; that is, the value of the sideslip angle is reduced in proportion to the decrease in slope of the lateral-force curve with sideslip angle. The variation of the effective sideslip angle β_{eff} used with the true sideslip angle β is shown in figure 20. It can be noted that the maximum lift on the vertical surface is assumed to occur at a sideslip angle of 25°. The transverse load factors have also been corrected for maximum lift and nonlinearity in the side-force curve in a similar manner.

It is indicated in figures 20 to 23 that the side loads obtainable in fishtail and rolling pull-out maneuvers are considerably greater than those obtained in the tests in service operations. For the F-86 airplane it can be seen in figure 22 that side loads were obtained in uncontrolled lateral oscillations which were equal in magnitude to those obtained in controlled maneuvers.

From the calculations of fishtail and rolling pull-out maneuvers for the F-86 airplane it is indicated that the largest side loads are produced in fishtail maneuvers at the higher speeds. Below an airspeed of about 330 knots, however, it is indicated that the rolling pull-out is the critical maneuver. The abrupt increase in side load in rolling pull-outs at these speeds for the particular airplane is caused by the maneuver being performed near maximum lift where the lateral derivatives have large changes with angle of attack.

Yawing velocity and acceleration: The maximum yawing velocities for the F-86A and F-84G airplanes are shown in figures 24 and 25, respectively, and the yawing angular accelerations are shown in figures 26 and 27, respectively. As was the case for the other lateral parameters, the maximum values of yawing velocity and acceleration obtained in the service tests were considerably below the maximum calculated values except for the yawing velocities in the calculated rolling pull-out maneuver for the F-86 airplane. (See fig. 24.) In this case the maximum yawing velocities obtained in the service tests approached those calculated for the rolling pull-out maneuver at the highest speeds. Again it can be noted in figures 24 and 26 that the calculated results indicate that the highest yawing velocities and accelerations are obtained in fishtail maneuvers at high speeds but that rolling pull-outs may result in higher values at lower speeds.

CONCLUDING REMARKS

From the results of this paper it is indicated that the service pilots in general made use of the static capabilities of their airplanes over most of the speed range as limited by control stops or control forces. The maximum response obtained in these service training operations, however, was considerably less than the theoretically obtainable maximum dynamic response. It is indicated that the pilots have a tendency to maneuver the airplane longitudinally near its natural frequency.

The results of the calculations of maximum dynamic response indicate that pitching accelerations greater than 16 radians per second per second are theoretically within the range of pilot and airplane capabilities for the F-86 airplane whereas the highest value obtained in the present tests was about 2 radians per second per second. For lateral maneuvers it is indicated that the highest vertical-tail loads for the F-86 airplane would generally be obtained in fishtail maneuvers; however, when rolling pull-out maneuvers were made near the maximum lift coefficient the vertical-tail loads obtained could be considerably greater than those obtained in fishtail maneuvers. The transverse load factors measured in the present tests were much less than those theoretically obtainable.

Langley Aeronautical Laboratory,
National Advisory Committee for Aeronautics,
Langley Field, Va., April 29, 1955.

REFERENCES

1. Mayer, John P., Hamer, Harold A., and Huss, Carl R.: A Study of the Use of Controls and the Resulting Airplane Response During Service Training Operations of Four Jet Fighter Airplanes. NACA RM L53I28, 1954.

2. Anderson, Seth B., and Bray, Richard S.: A Flight Evaluation of the Longitudinal Stability Characteristics Associated with the Pitch-Up of a Swept-Wing Airplane in Maneuvering Flight at Transonic Speeds. NACA RM A51I12, 1951.

3. Schmidt, Richard A., and Collins, Harold E.: Maneuvering Stability and Buffet Speeds of an F-86A With and Without 245, 165, and 120-Gallon External Fuel Tanks. Memo. Rep. No. MCRFT-2250, Air Materiel Command, Flight Test Div., U. S. Air Force, Oct. 14, 1949.

4. Schmidt, Richard A., McAuly, Walter J., Jr., and Collins, Harold E.: Partial Phase IV Stability and Control Flight Tests of F-86A, USAF No. 47-610. Memo. Rep. No. MCRFT-2315, Air Materiel Command, Flight Test Div., U. S. Air Force, Dec. 19, 1950.

5. Anon.: Report of Service Acceptance Trials on Models F2H-2 and F2H-2N Aircraft (TED No. BIS 21124). Vol. II, Board of Inspection and Survey, U. S. Navy, 1951.

6. Crane, H. L., Beckhardt, A. R., and Matheny, C. E.: Flight Measurements of the Lateral Stability and Control Characteristics of a High-Speed Fighter Airplane. NACA RM L52B14, 1952.

7. Smith, Donald R., and Curtis, Thomas H.: Phase IV Stability and Control Flight Tests of the F-84E Airplane, USAF No. 49-2028. Memo. Rep. No. FTD-52-6, Air Force Flight Test Center (Edwards, Calif.), Apr. 23, 1952.

8. Pearson, Richard E., and Knight, John J.: Phase IV Stability and Control Flight Tests of the F-94A Aircraft, USAF No. 49-2500. Memo. Rep. No. WCT-52-10, Wright Air Dev. Center, U. S. Air Force, May 16, 1952.

9. Anon.: Specification For Flying Qualities of Piloted Airplanes. NAVAER SR-119B, Bur. Aero., June 1, 1948.

10. Anon.: Flying Qualities of Piloted Airplanes. USAF Spec. No. 1815-B, June 1, 1948.

11. Pearson, Henry A., McGowan, William A., and Donegan, James J.: Horizontal Tail Loads in Maneuvering Flight. NACA Rep. 1007, 1951. (Supersedes NACA TN 2078.)

12. Anon.: Airplane Strength and Rigidity. NAVAER SS-1C, Bur. Aero., Aug. 1, 1946.

13. Matheny, Cloyce E.: Maximum Pitching Angular Accelerations of Airplanes Measured in Flight. NACA TN 2103, 1950.

14. Anon.: Compilation of CAA Rules, Policies, and Interpretations Which Apply to Civil Air Regulation 3. Civil Aero. Manual 3, Supp. No. 5, CAA, U. S. Dept. Commerce, Mar. 8, 1950.

15. Bouton, Innes: Maneuvering Horizontal Tail Loads. Jour. Aero. Sci. (Readers' Forum), vol. 16, No. 7, July 1949, pp. 440-441.

16. Donegan, James J.: Matrix Methods for Determining the Longitudinal-Stability Derivatives of an Airplane From Transient Flight Data. NACA Rep. 1169, 1954. (Supersedes NACA TN 2902.)

17. Anon.: Aerodynamic Load Calculations for a Jet Propeller Fighter Airplane (Monoplace) AAF Model F-86A. Rep. No. NA-46-1174, North American Aviation, Inc. Feb. 7, 1949.

18. Morrill, Charles P., Jr., and Boddy, Lee E.: High-Speed Stability and Control Characteristics of a Fighter Airplane Model With a Swept-Back Wing and Tail. NACA RM A7K28, 1948.

19. Jaquet, Byron M.: Calculated Lateral Frequency Response and Lateral Oscillatory Characteristics for Several High-Speed Airplanes in Various Flight Conditions. NACA RM L53J01, 1953.

20. Stone, Ralph W., Jr.: An Analytical Study of Sideslip Angles and Vertical-Tail Loads in Rolling Pullouts as Affected by Some Characteristics of Modern High-Speed Airplane Configurations. NACA RM L53G21, 1953.

21. Triplett, William C., and Brown, Stuart C.: Lateral and Directional Dynamic-Response Characteristics of a 35° Swept-Wing Airplane As Determined From Flight Measurements. NACA RM A52I17, 1952.

22. Donegan, James J., Robinson, Samuel W., Jr., and Gates, Ordway B.: Determination of Lateral-Stability Derivatives and Transfer-Function Coefficients From Frequency-Response Data for Lateral Motions. NACA TN 3083, 1954.

TABLE I.- DIMENSIONS AND PHYSICAL CHARACTERISTICS OF THE TEST AIRPLANES

Component	Item	Unit	Airplane			
			F-86A	F2H-2	F-84G	F-94B
Wing	Serial number		{USAF 48-227 / USAF 49-1265}	BuAero number 123256	USAF 51-835	USAF 51-5380A
	Total area (including portion covered by fuselage)	sq ft	287.9	294.1	261.0	238.0
	Span (without tip tanks)	in.	445.4	500.8	438.8	451.3
	Mean aerodynamic chord	in.	97.0	88.4	88.8	80.6
	Lateral location of mean aerodynamic chord normal to fuselage reference line	in.	98.7	111.0	98.3	92.0
	Vertical location of mean aerodynamic chord normal to and below fuselage reference line	in.	25.7	0.4	2.4	13.4
	Distance from nose to leading edge of mean aerodynamic chord	in.	164.3	197.0	169.6	210.9
	Aspect ratio		4.79	5.89	5.10	5.96
	Taper ratio, $\frac{\text{Tip chord}}{\text{Root chord}}$		0.51	0.52	0.57	0.38
	Sweepback of 25-percent-chord line	deg	35.2	-------	-------	------
	Incidence of root chord	deg	1.0	-0.5	0.0	1.0
	Incidence of tip chord	deg	-1.0	-0.5	-2.0	-0.5
	Dihedral	deg	3.0	3.0	5.0	3.5
	Root airfoil section		NACA 0012-64 (modified)	NACA 65_1-212	RA,45-1512-.9 (12 percent thick)	NACA 65_{112}-213
	Tip airfoil section		NACA 0011-64 (modified)	NACA 63-209	RA,45-1512-.9 (12 percent thick)	NACA 65_{112}-213
Aileron	Total area (one)	sq ft	18.6	9.4	16.1	8.8
	Static limits of travel	deg	{Up 15 / Down 15}	Up 20 Down 20	Up 17.2 Down 15.2	Up 20 Down 20
Horizontal tail	Total area (including portion covered by fuselage)	sq ft	35.0	69.8	48.4	47.8
	Span	in.	153.0	224.7	179.3	199.0
	Mean aerodynamic chord	in.	34.7	47.4	40.1	38.2
	Lateral location of mean aerodynamic chord normal to fuselage reference line	in.	38.5	49.6	41.5	38.5
	Vertical location of mean aerodynamic chord normal to and above fuselage reference line	in.	23.5	58.0	27.5	28.4
	Tail length (25 percent of wing M.A.C. to 25 percent of horizontal-tail M.A.C.)	in.	222.3	203.1	217.0	190.5
	Aspect ratio		4.65	4.65	4.65	5.75
	Taper ratio, $\frac{\text{Tip chord}}{\text{Root chord}}$		0.45	0.60	0.56	0.36
	Sweepback of 25-percent-chord line	deg	34.6	------	------	-------
	Incidence	deg	Adjustable	0.4	0.0	0.5
	Dihedral	deg	10.0	0.0	5.0	0.0
	Airfoil section		NACA 0010-64	NACA $65_{(10)}$-011	RA,40-020	NACA 65-010
Elevator	Total area (one)	sq ft	5.1	9.4	8.5	4.4
	Static limits	deg	{Up 35 / Down 17.5}	Up 15 Down 15	Up 25 Down 10	Up 38 Down 17.5

TABLE I.- DIMENSIONS AND PHYSICAL CHARACTERISTICS OF THE TEST AIRPLANES - Concluded

Component	Item	Unit	Airplane			
			F-86A	F2H-2	F-84G	F-84B
Stabilizer	Leading-edge limits of travel	deg	Up 1.3 Down 10	Fixed	Fixed	Fixed
Vertical tail	Total area (including portion above fuselage and excluding dorsal or ventral area)	sq ft	33.4	38.9	30.9	22.5
	Span (from fuselage contour)	in.	90.2	86.0	86.0	77.0
	Mean aerodynamic chord	in.	57.5	67.3	63.0	48.3
	Vertical location of mean aerodynamic chord above fuselage contour	in.	38.5	37.6	28.3	25.5
	Vertical location of mean aerodynamic chord normal to and above fuselage reference line	in.	55.7	77.6	43.5	56.1
	Tail length (25 percent of wing M.A.C. to 25 percent of vertical-tail M.A.C.)	in.	202.3	205.4	218.3	193.5
	Aspect ratio		1.74	1.34	2.23	1.83
	Taper ratio, $\frac{\text{Tip chord}}{\text{Root chord}}$		0.36	0.45	0.39	0.40
	Sweepback of 25-percent-chord line	deg	35.0	------	------	------
	Airfoil section		NACA 0011-64	NACA 65(10)-011	RA,40-010	NACA 65-010
Rudder	Total area	sq ft	8.1	10.1	10.0	5.3
	Static limits	deg	Right 27.5 Left 27.5	Right 20 Left 20	Right 23.5 Left 23.5	Right 30 Left 30
Fuselage	Total length (excluding nose boom)	in.	412.4	481.8	461.4	481.3
	Maximum width	in.	60.0	46.9	49.9	56.0
	Frontal area (excluding canopy)	sq ft	20.0 (approx.)	15.7	17.0	17.0 (approx.)
Speed brakes	Total effective frontal area	sq ft	8.6	11.6 including cutouts	3.4	5.0
Tip tanks	Weight empty (one)	lb	----------	200	178	190
	Capacity (one)	gal	----------	200	230	230
Weight and location of center of gravity (full service)	Measured airplane weight	lb	[a]14,220	[b]17,940	[b]15,440	[a]13,160
	Center-of-gravity location corresponding to above weight	percent M.A.C.	20.8	26.8	23.8	27.5
Estimated moments of inertia for weight as given	Corresponding weight	lb	[a]12,600	[b]16,520	[b]15,440	[a]13,650
	I_X (roll)	slug-ft^2	6,700	19,000	18,600	11,900
	I_Y (pitch)	slug-ft^2	16,500	26,300	21,300	26,600
	I_Z (yaw)	slug-ft^2	21,700	42,700	38,900	37,800
Powerplant			General Electric J-47	Westinghouse (two) J-34-WE-34	Allison J-35-A-29	Allison J-33-A-33 with afterburner

[a]No external tanks.
[b]Tip tanks on but empty.

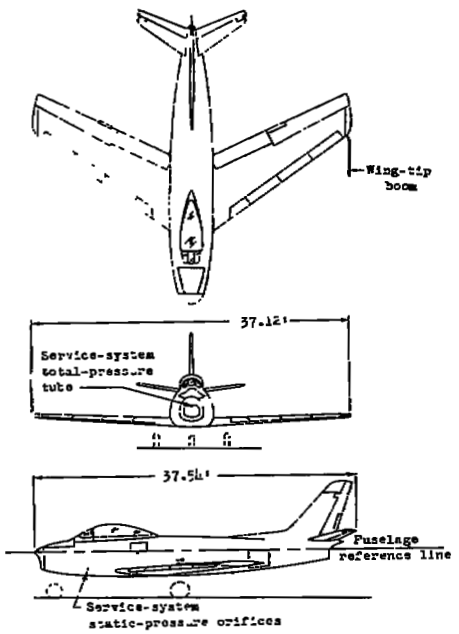

F-86A

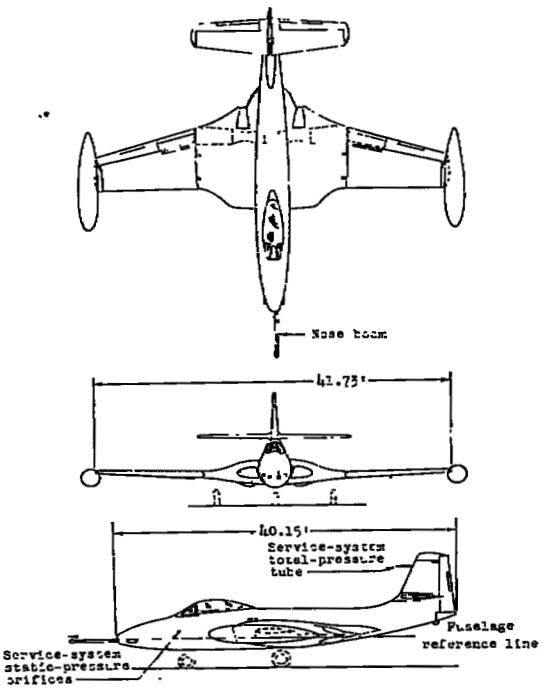

F2H-2

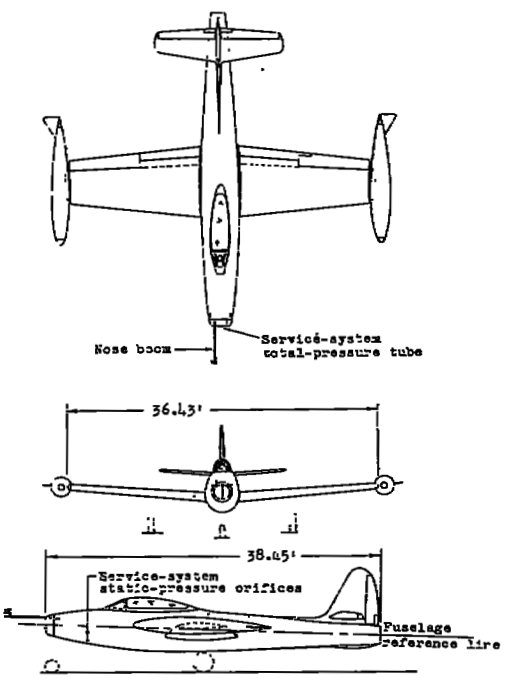

F-84G

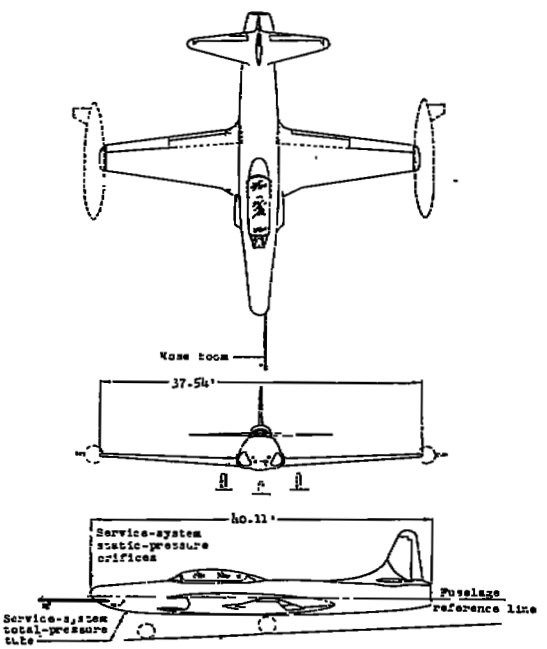

F-94B

Figure 1.- Three-view drawings of test airplanes.

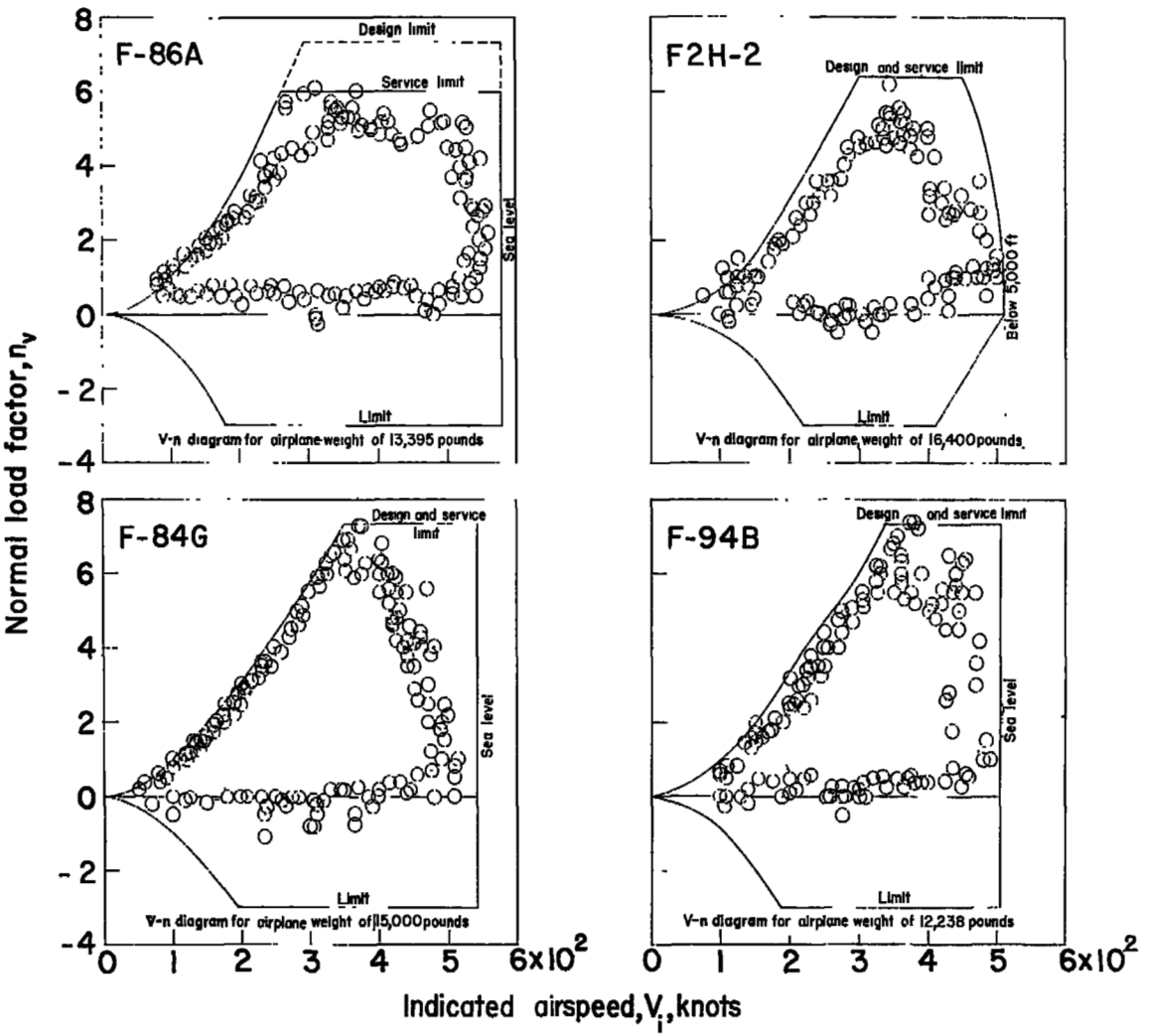

Figure 2.- Comparison of normal load factors with the airplane operational V-n diagram.

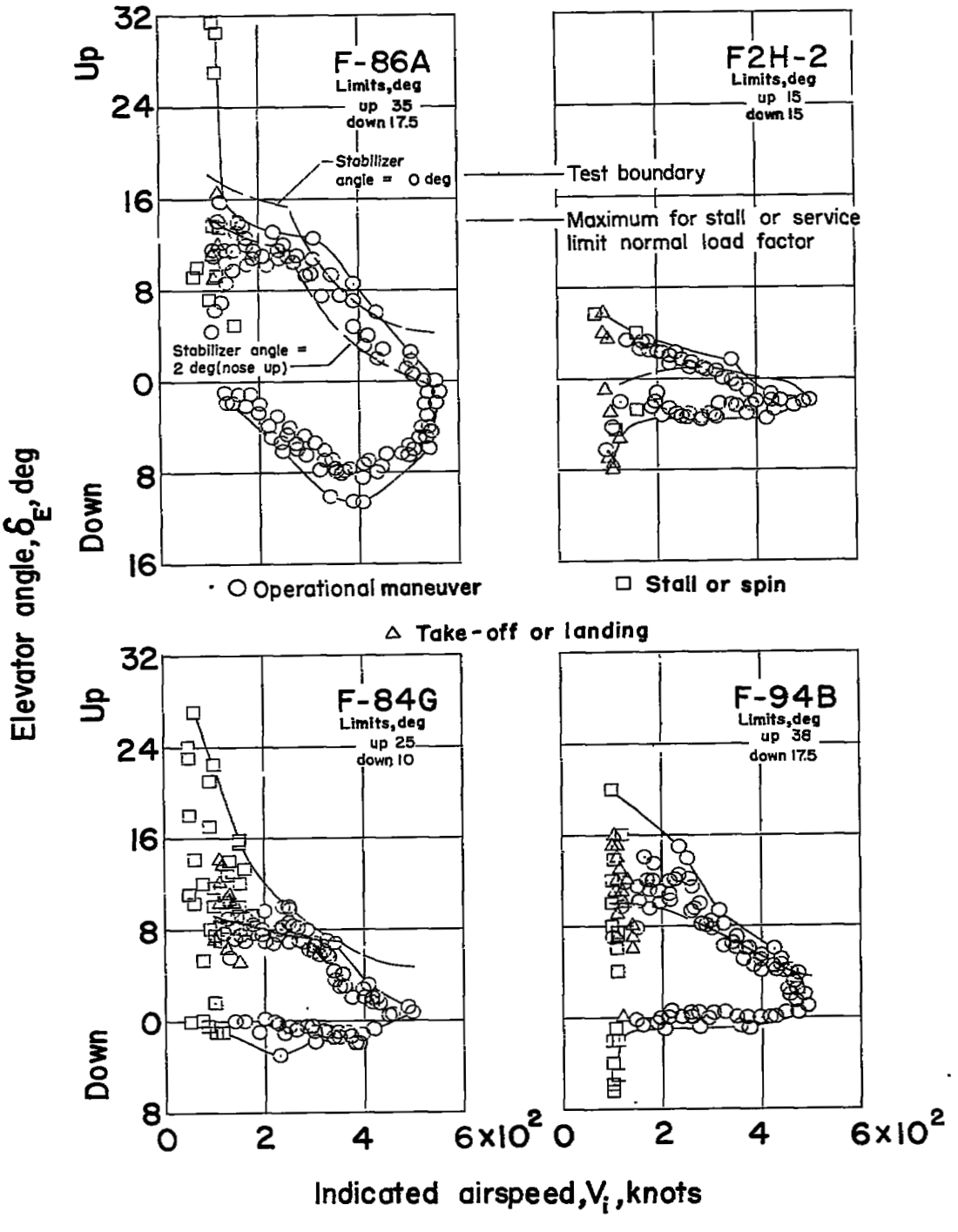

Figure 3.- Comparison of test results with maximum elevator angles needed to reach stall or the service limit normal load factor in gradual maneuvers.

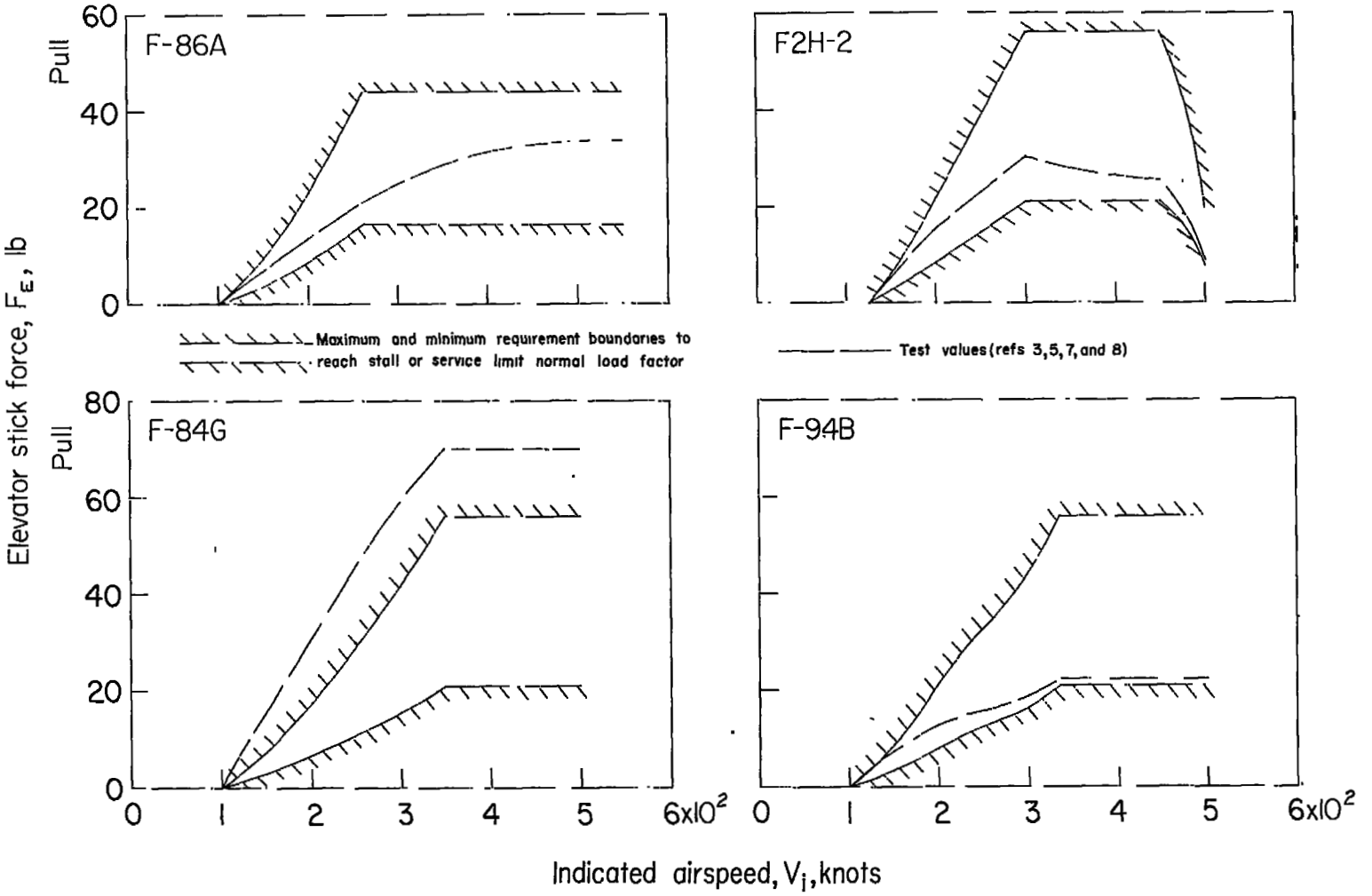

Figure 4.- Comparison of elevator stick forces needed to reach stall or the service limit normal load factor in gradual maneuvers with the maximum and minimum requirements.

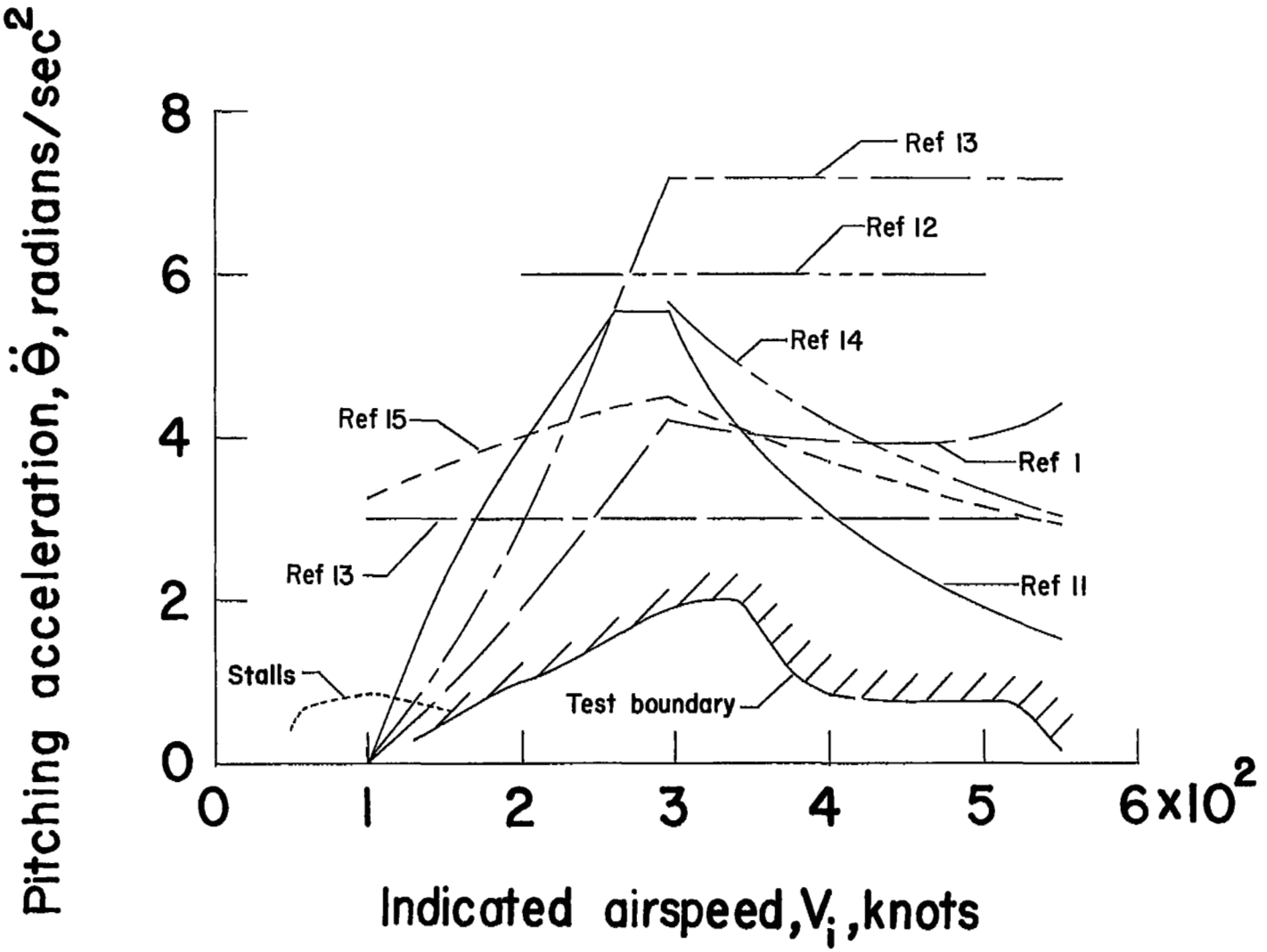

Figure 5.- Comparison of test results with various methods of calculating pitching accelerations.

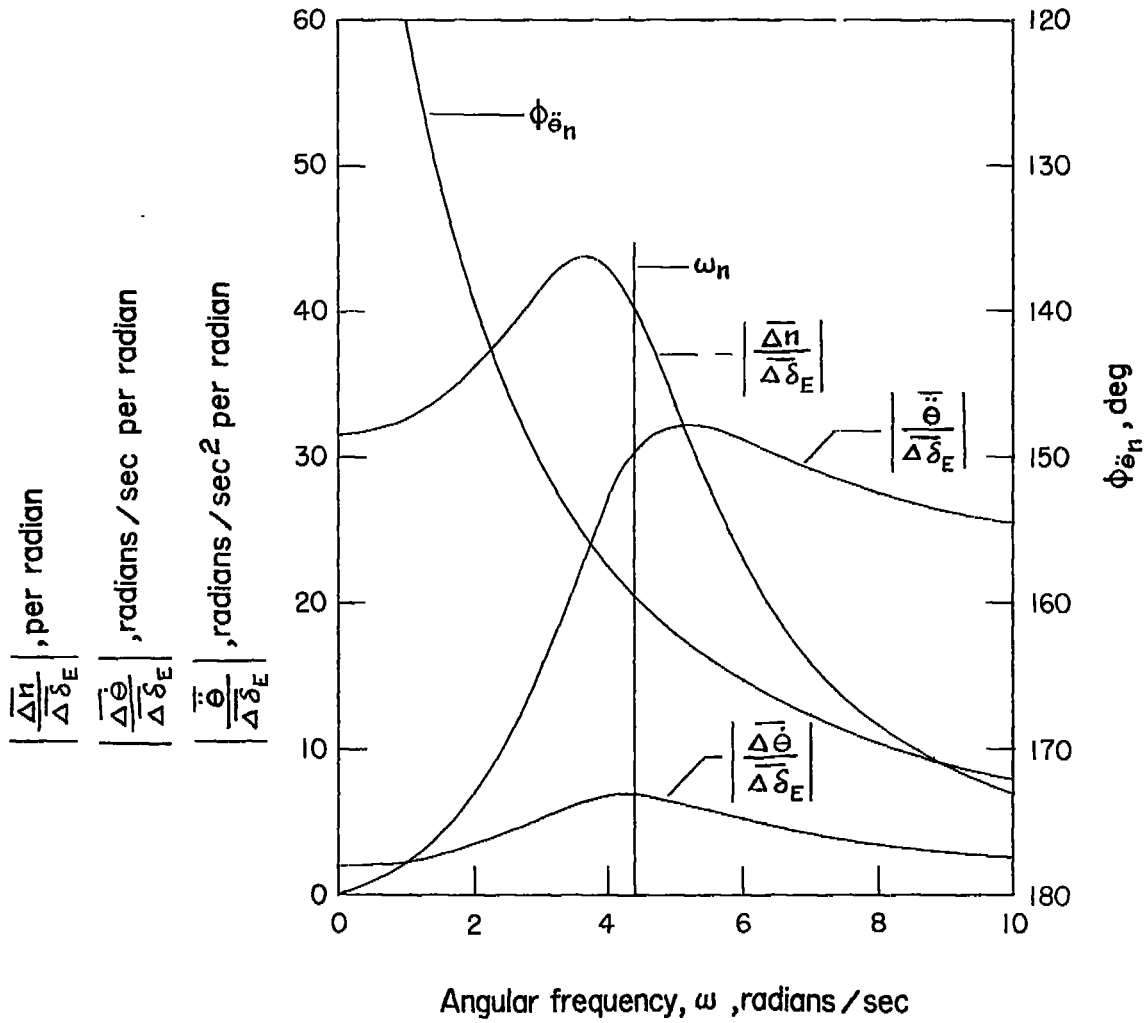

Figure 6.- Longitudinal frequency response of the F-86A airplane for an airspeed of 300 knots at sea level.

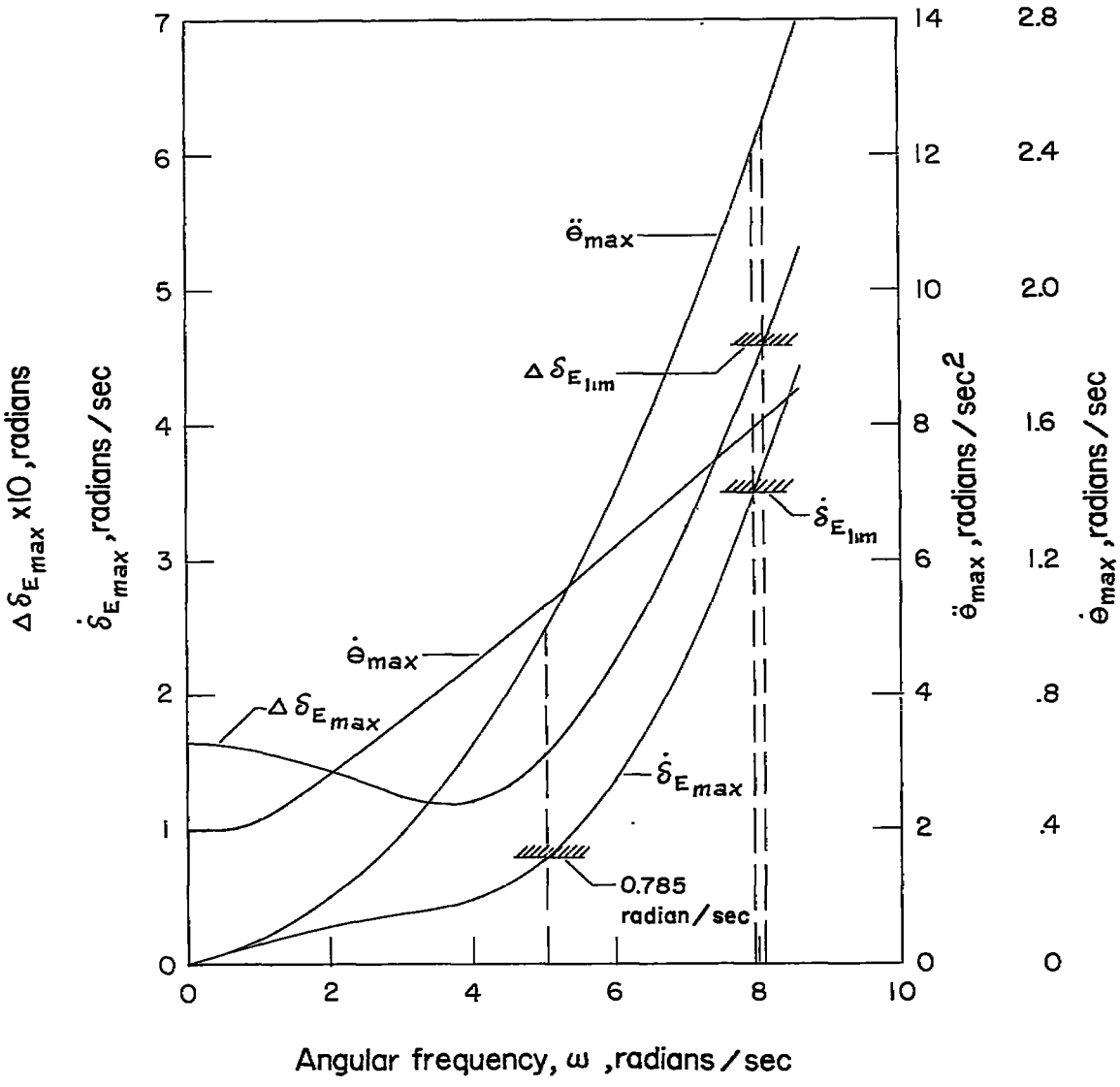

Figure 7.- Maximum control and response values calculated for the F-86A airplane maneuvering sinusoidally between the upper and lower limits of the design V-n diagram for an airspeed of 300 knots at sea level.

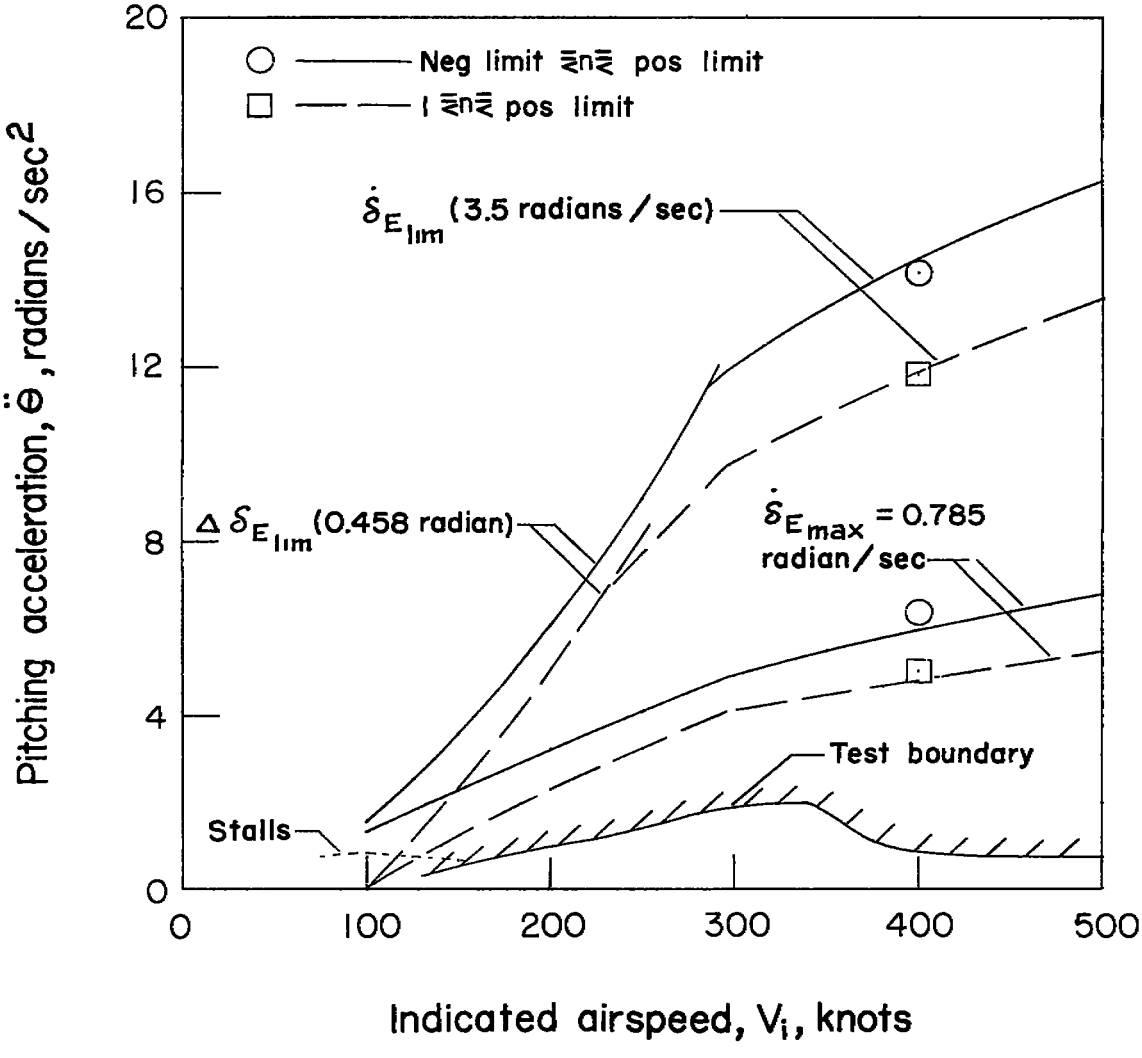

Figure 8.- Comparison of test results with maximum calculated pitching accelerations obtained by maneuvering the F-86A airplane sinusoidally within the V-n diagram at sea level. (Symbols are for altitude of 20,000 feet.)

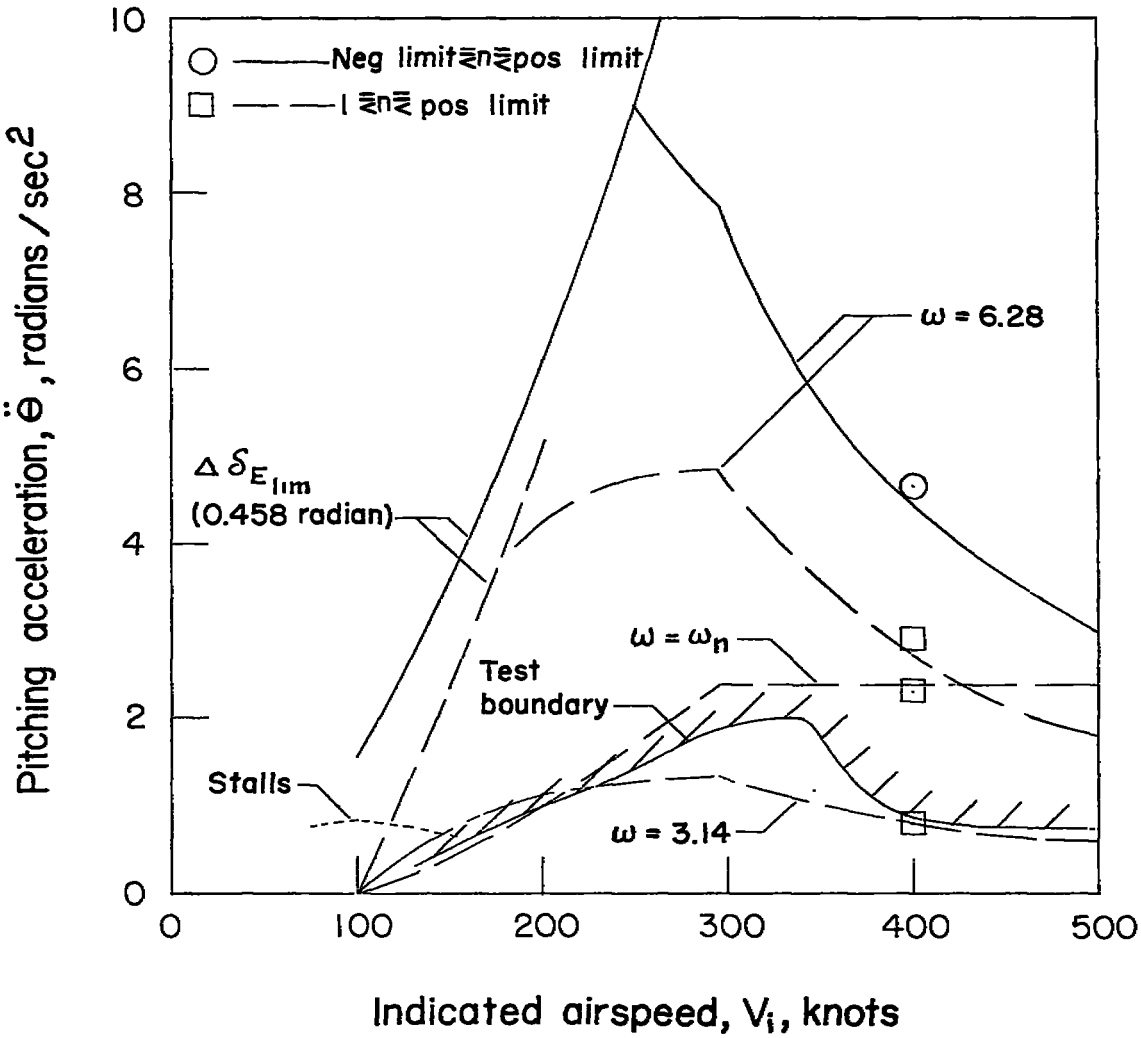

Figure 9.- Comparison of test results with maximum calculated pitching accelerations obtained by maneuvering the F-86A airplane sinusoidally within the V-n diagram at sea level. (Symbols are for altitude of 20,000 feet.)

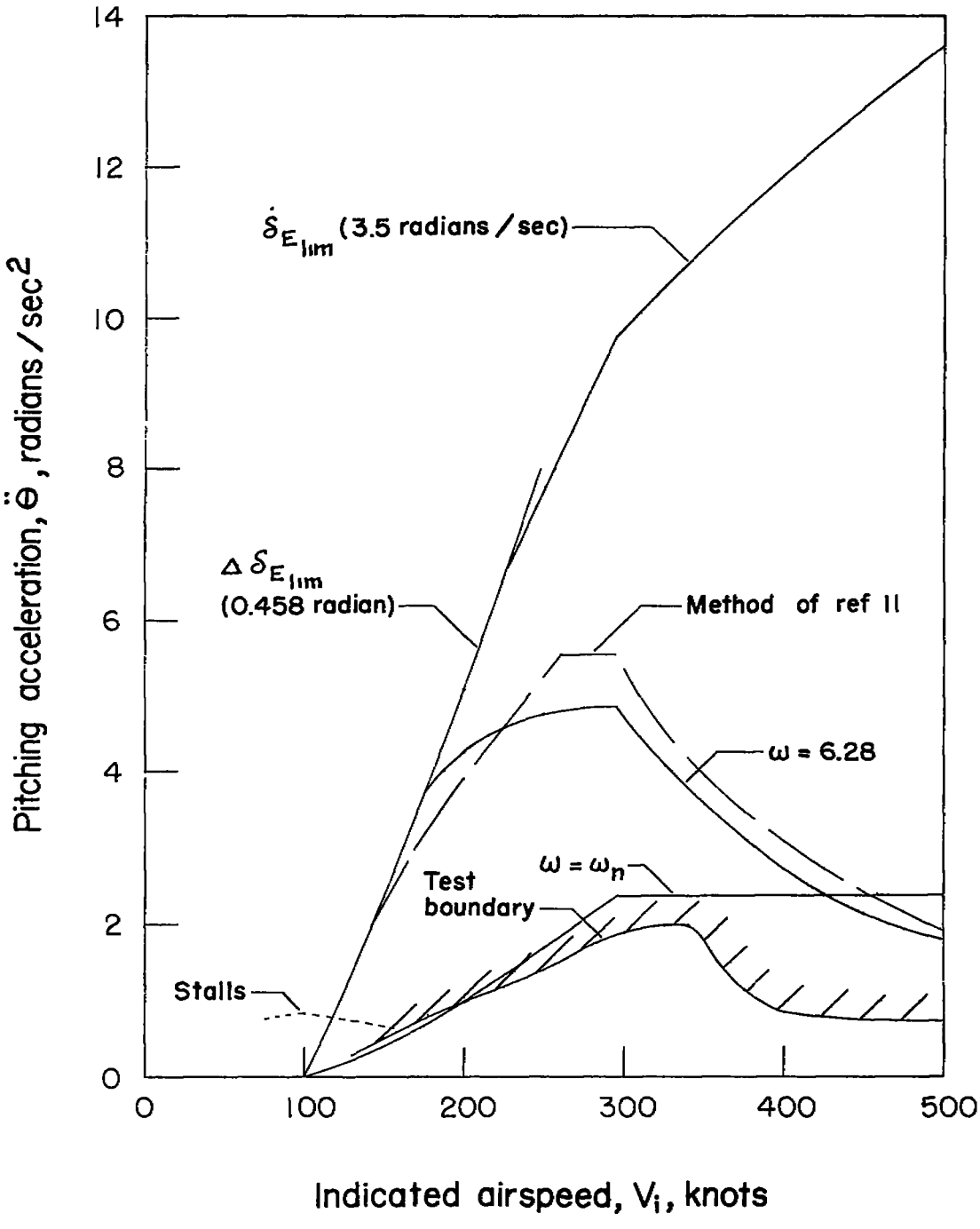

Figure 10.- Comparison of test results with maximum calculated pitching accelerations obtained by maneuvering the F-86A airplane sinusoidally between a load factor of 1 and the upper limit of the design V-n diagram at sea level.

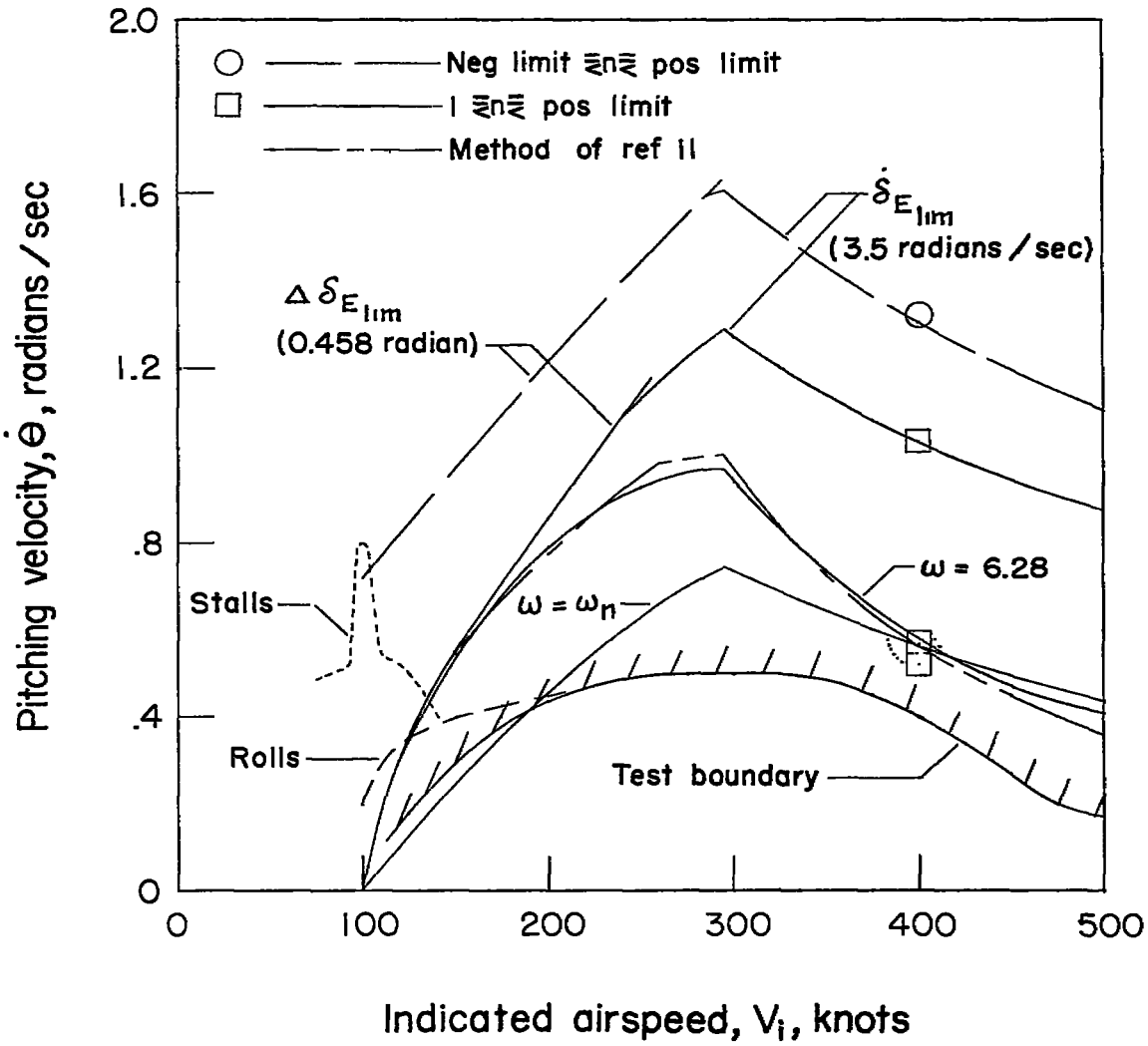

Figure 11.- Comparison of test results with maximum calculated pitching velocities obtained by maneuvering the F-86A airplane sinusoidally within the V-n diagram at sea level. (Symbols at 400 knots are for altitude of 20,000 feet.)

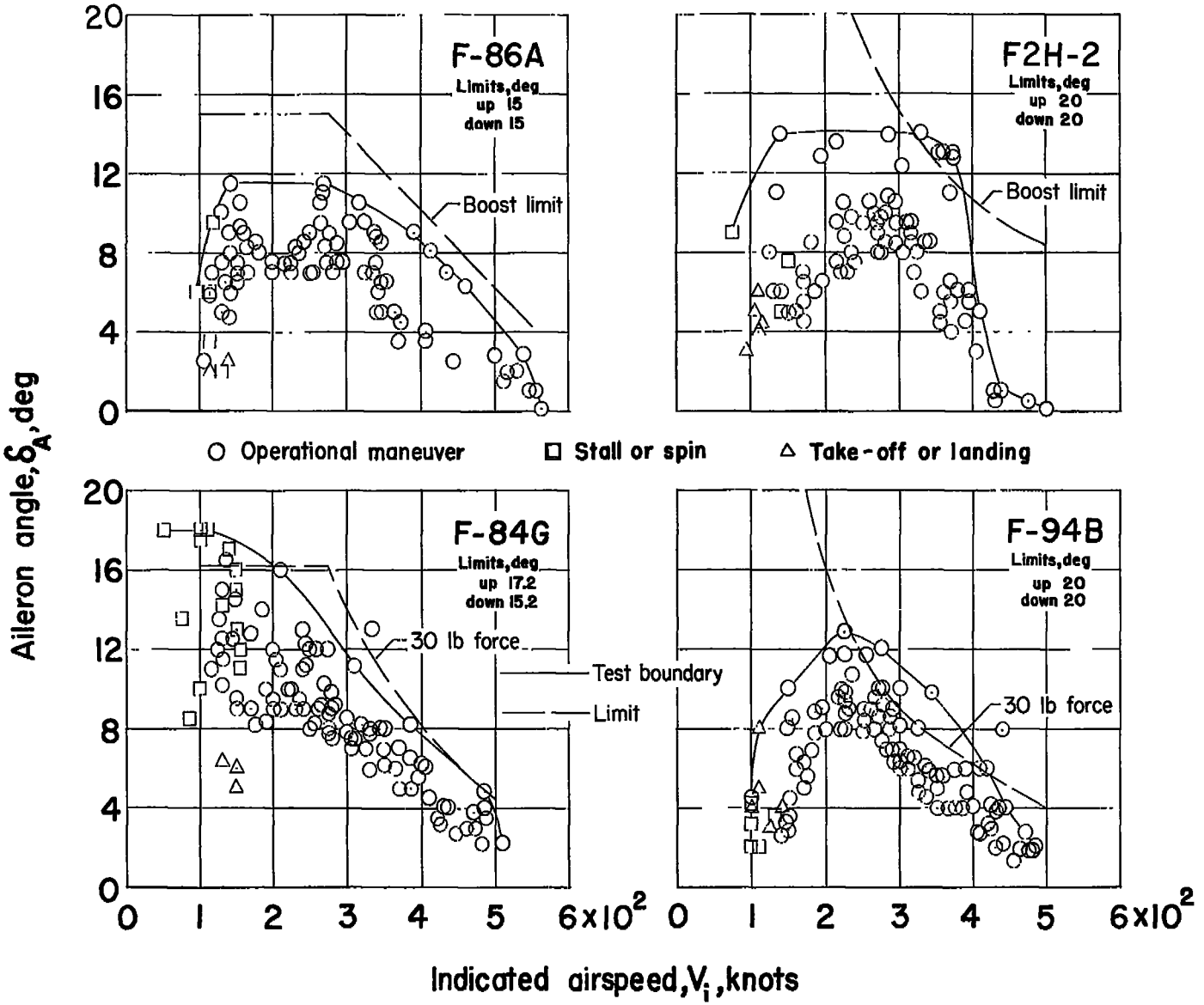

Figure 12.- Comparison of test results with maximum up or down aileron angles obtainable in abrupt aileron rolls.

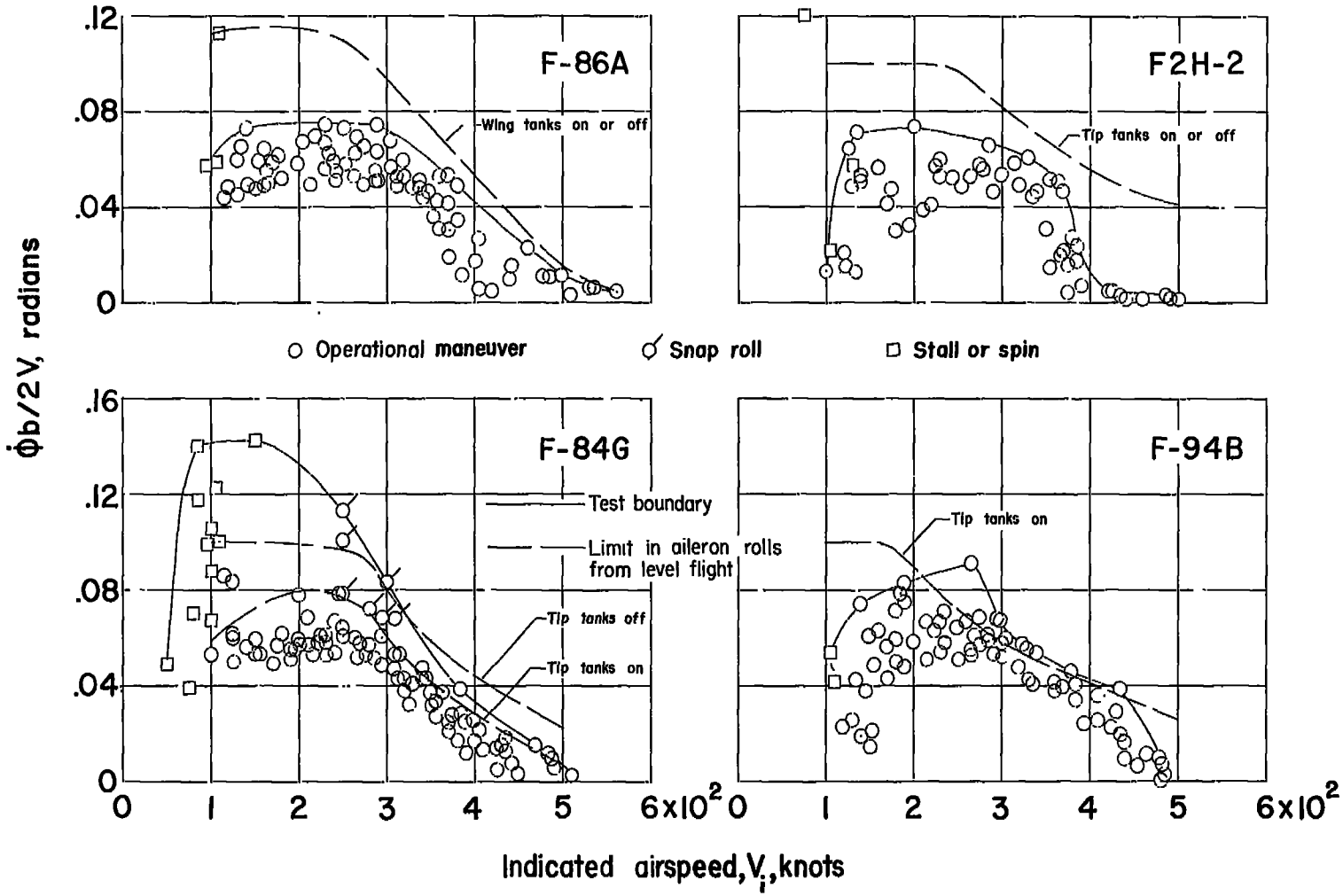

Figure 13.- Comparison of test results with maximum wing-tip helix angles obtainable in abrupt aileron rolls.

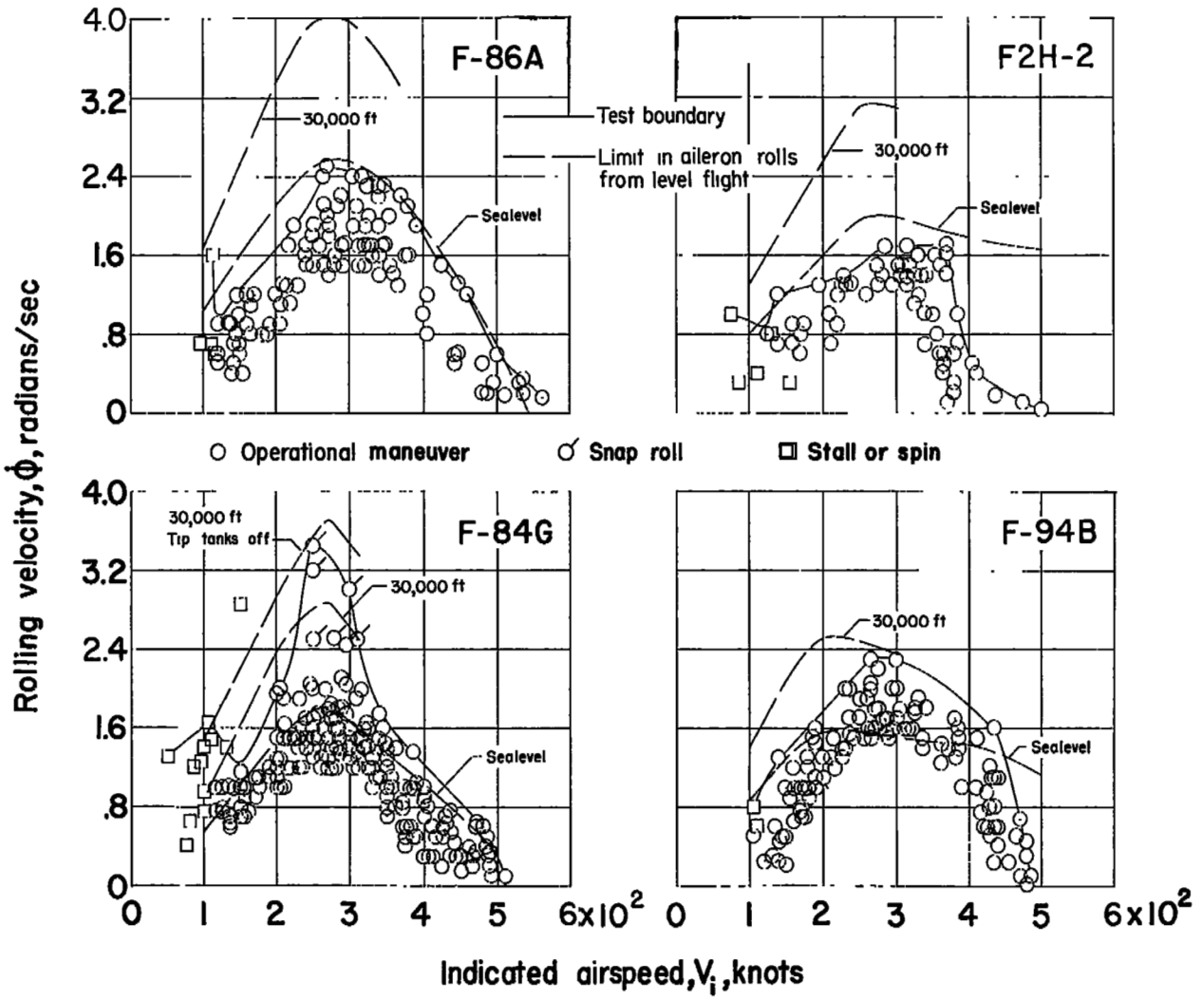

Figure 14.- Comparison of test results with maximum rolling velocities obtainable in abrupt aileron rolls.

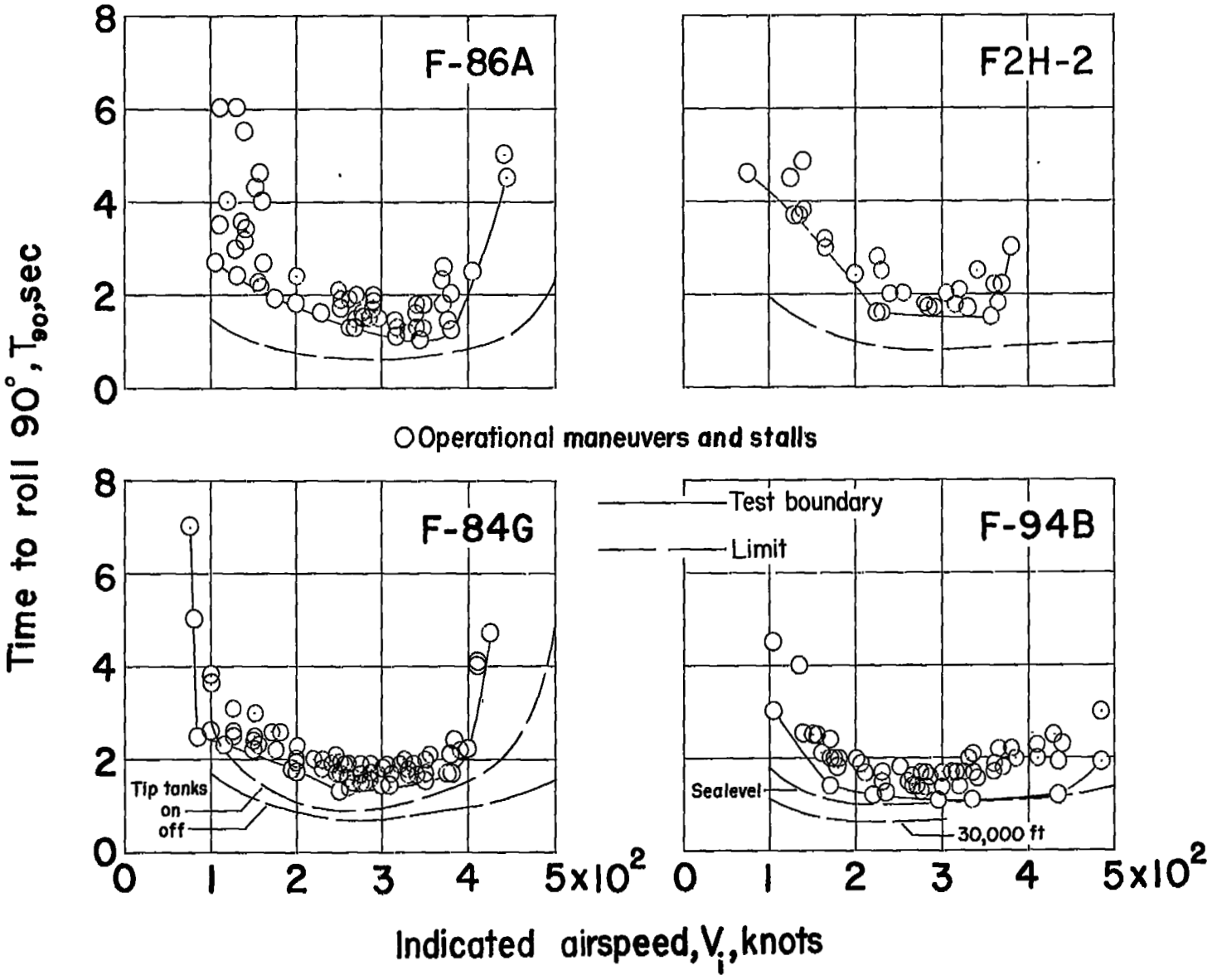

Figure 15.- Comparison of test results with calculated minimum times to roll 90° in abrupt aileron rolls at sea level.

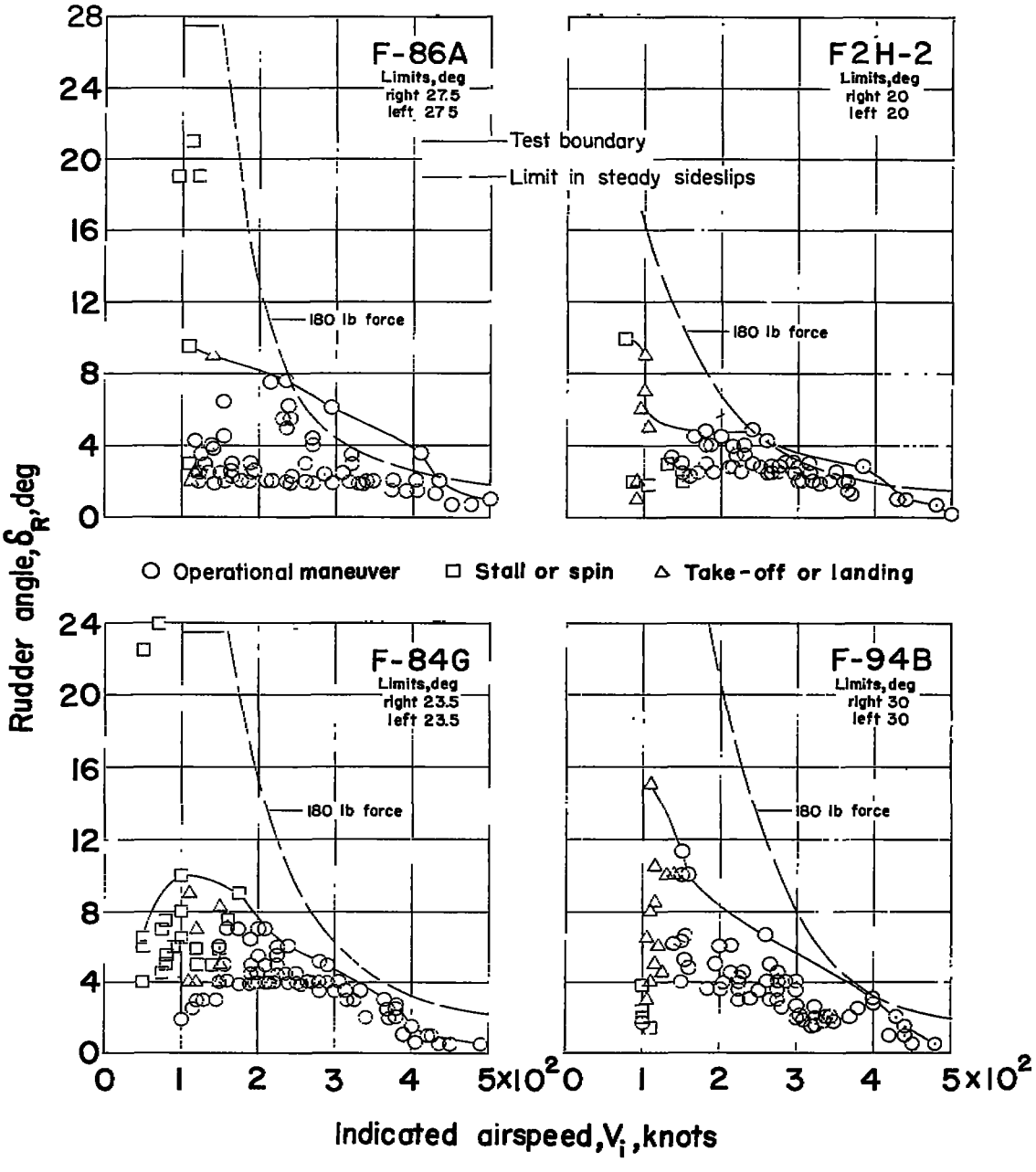

Figure 16.- Comparison of test results with maximum rudder angles obtainable in steady sideslips using maximum control force of 180 pounds.

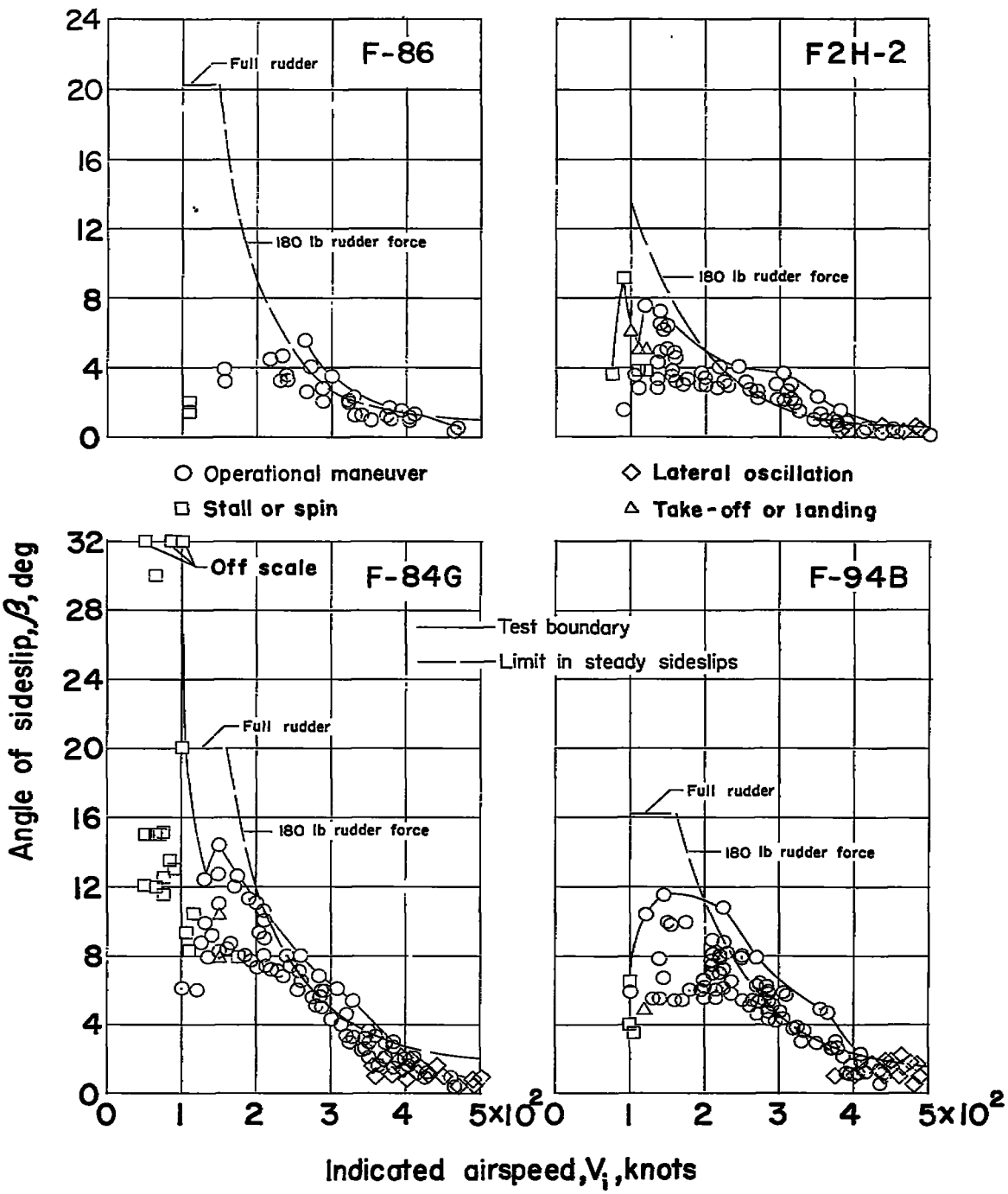

Figure 17.- Comparison of test results with maximum angles of sideslip obtainable in steady sideslips using maximum rudder control force of 180 pounds.

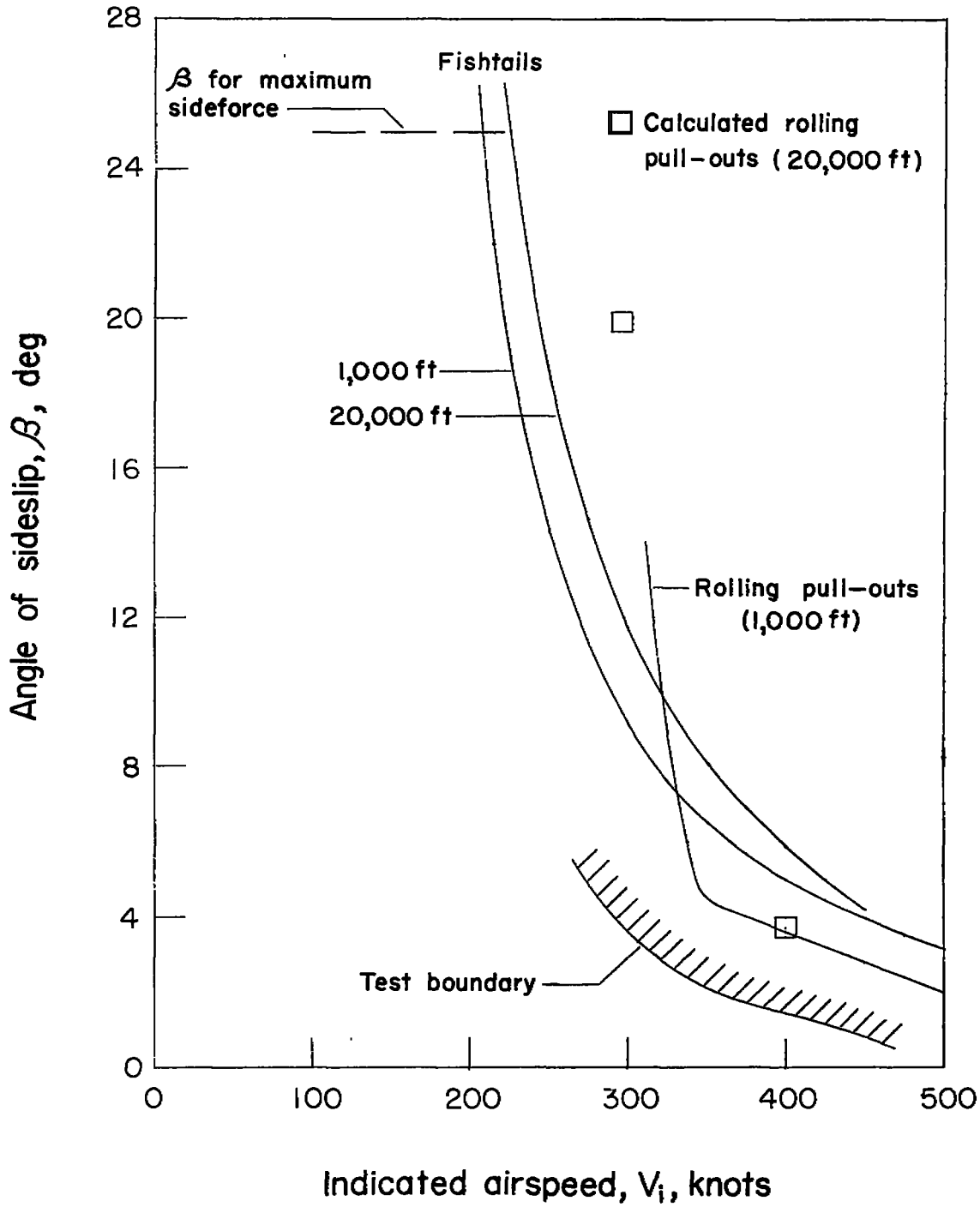

Figure 18.- Comparison of test results for the F-86A airplane with maximum calculated values of sideslip during fishtail and rolling pull-out maneuvers.

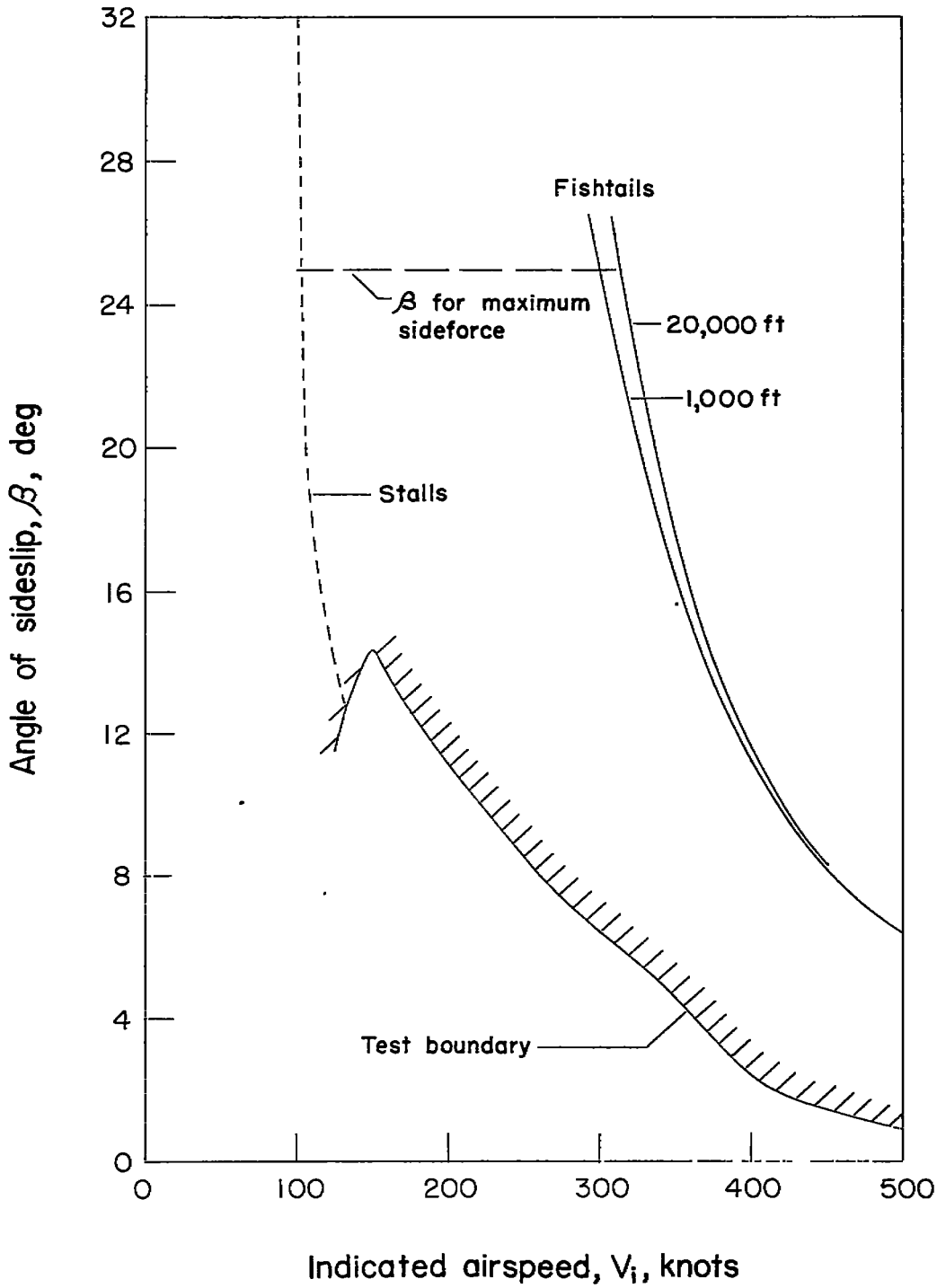

Figure 19.- Comparison of test results for the F-84 airplane with maximum calculated values of sideslip during fishtail maneuvers.

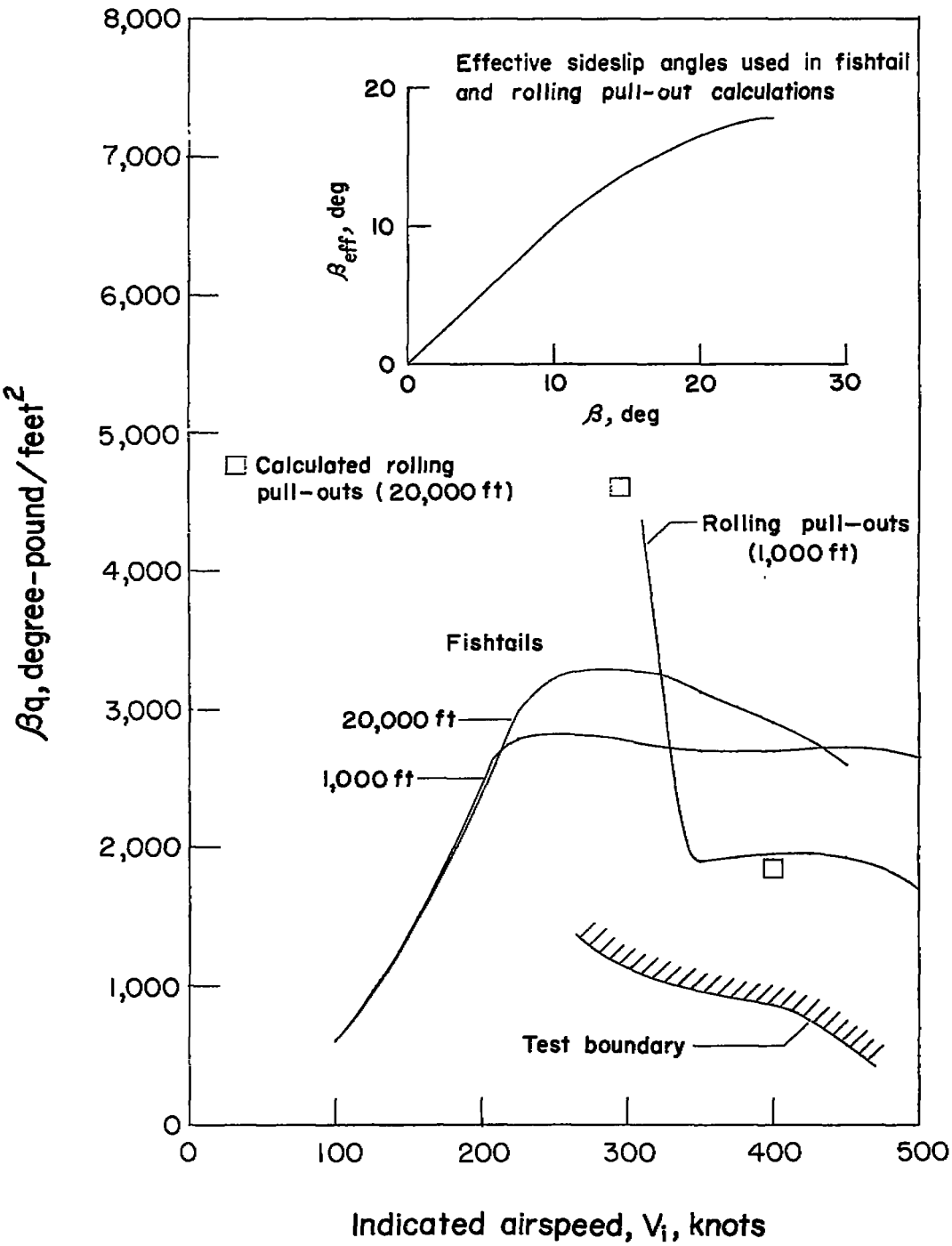

Figure 20.- Comparison of test results for the F-86A airplane with maximum calculated values of vertical-tail load parameter βq during fishtail and rolling pull-out maneuvers.

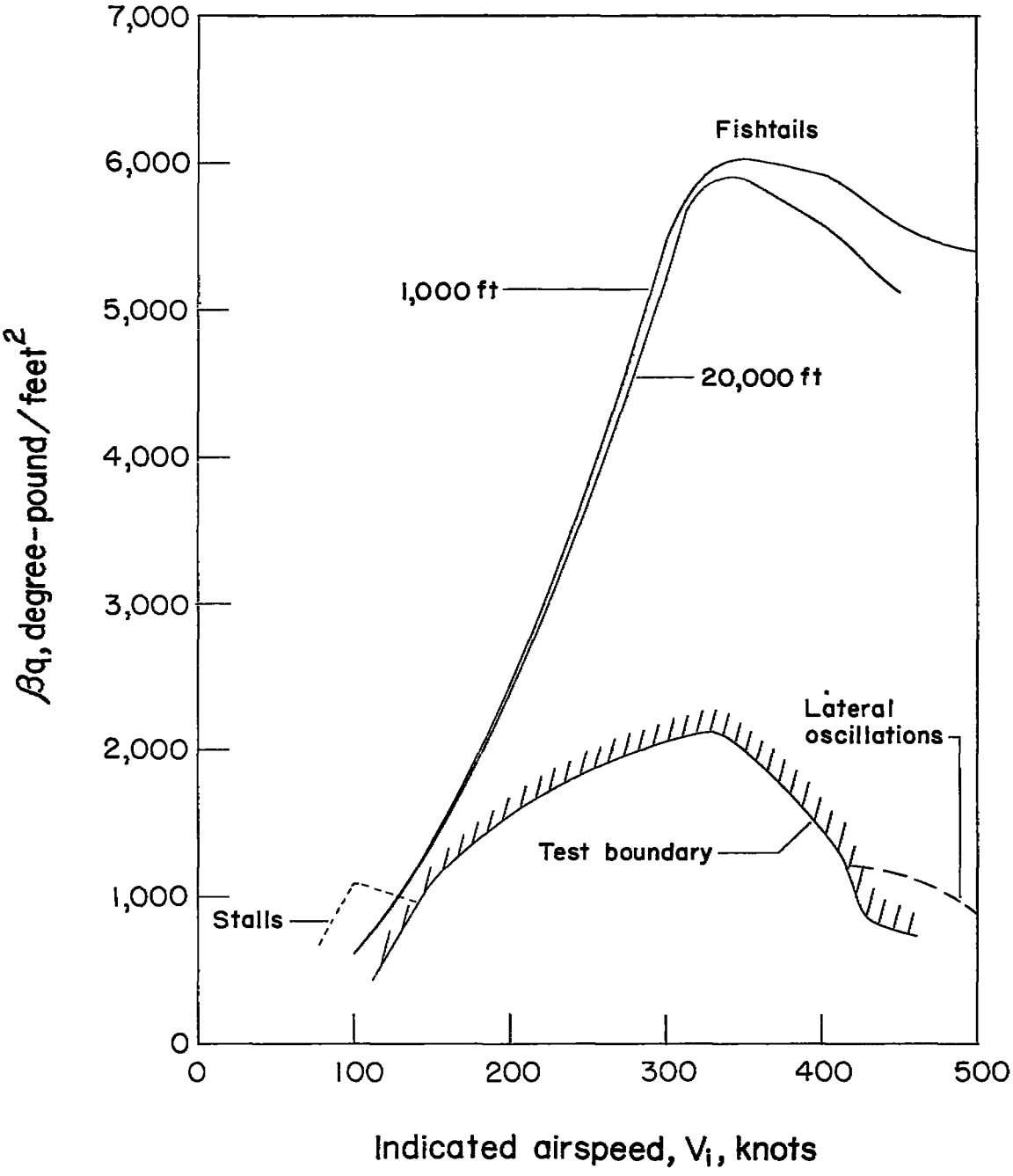

Figure 21.- Comparison of test results for the F-84 airplane with maximum calculated values of vertical-tail load parameter βq during fishtail maneuvers.

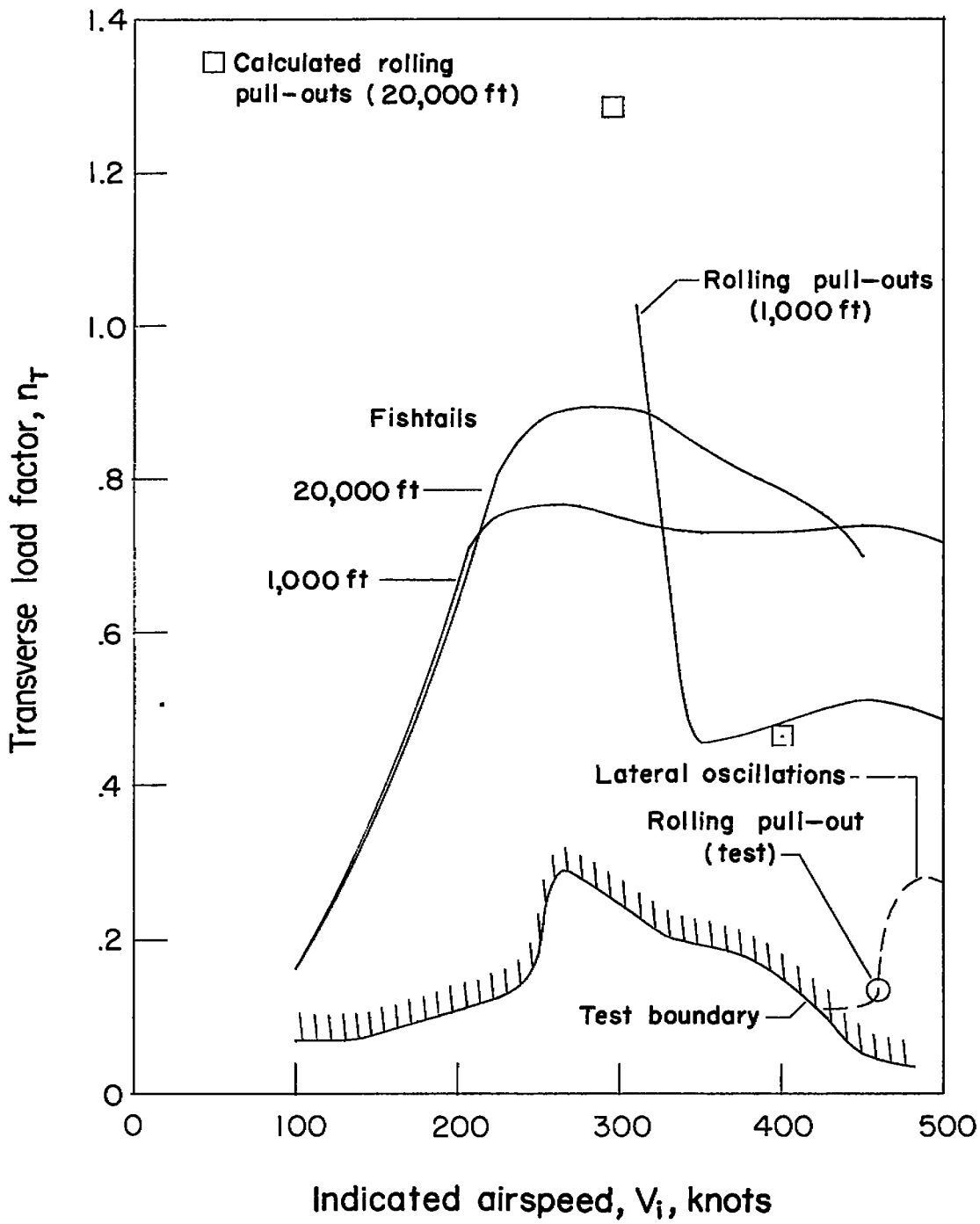

Figure 22.- Comparison of test results for the F-86A airplane with maximum calculated values of transverse load factor during fishtail and rolling pull-out maneuvers.

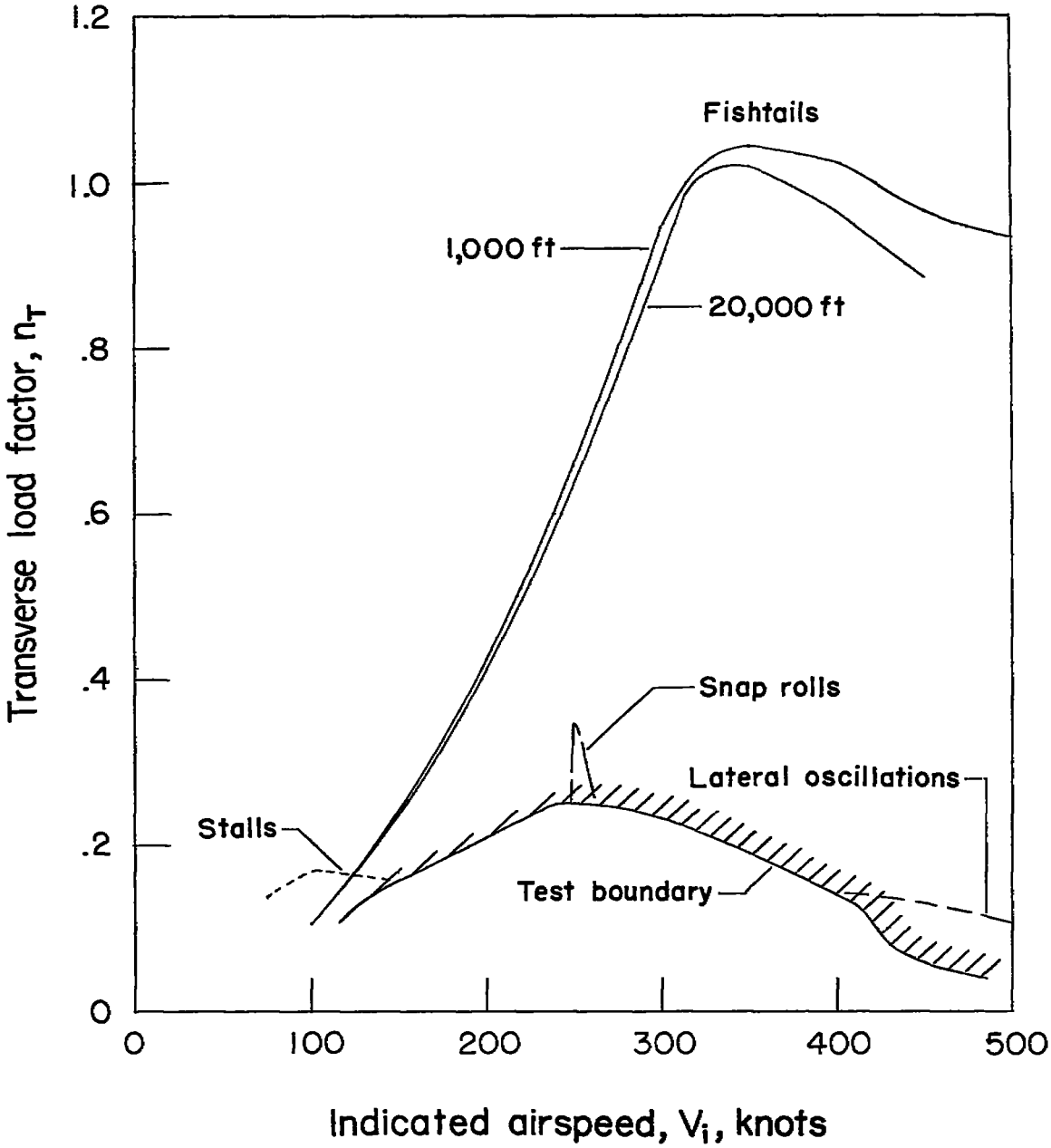

Figure 23.- Comparison of test results for the F-84 airplane with maximum calculated values of transverse load factor during fishtail maneuvers.

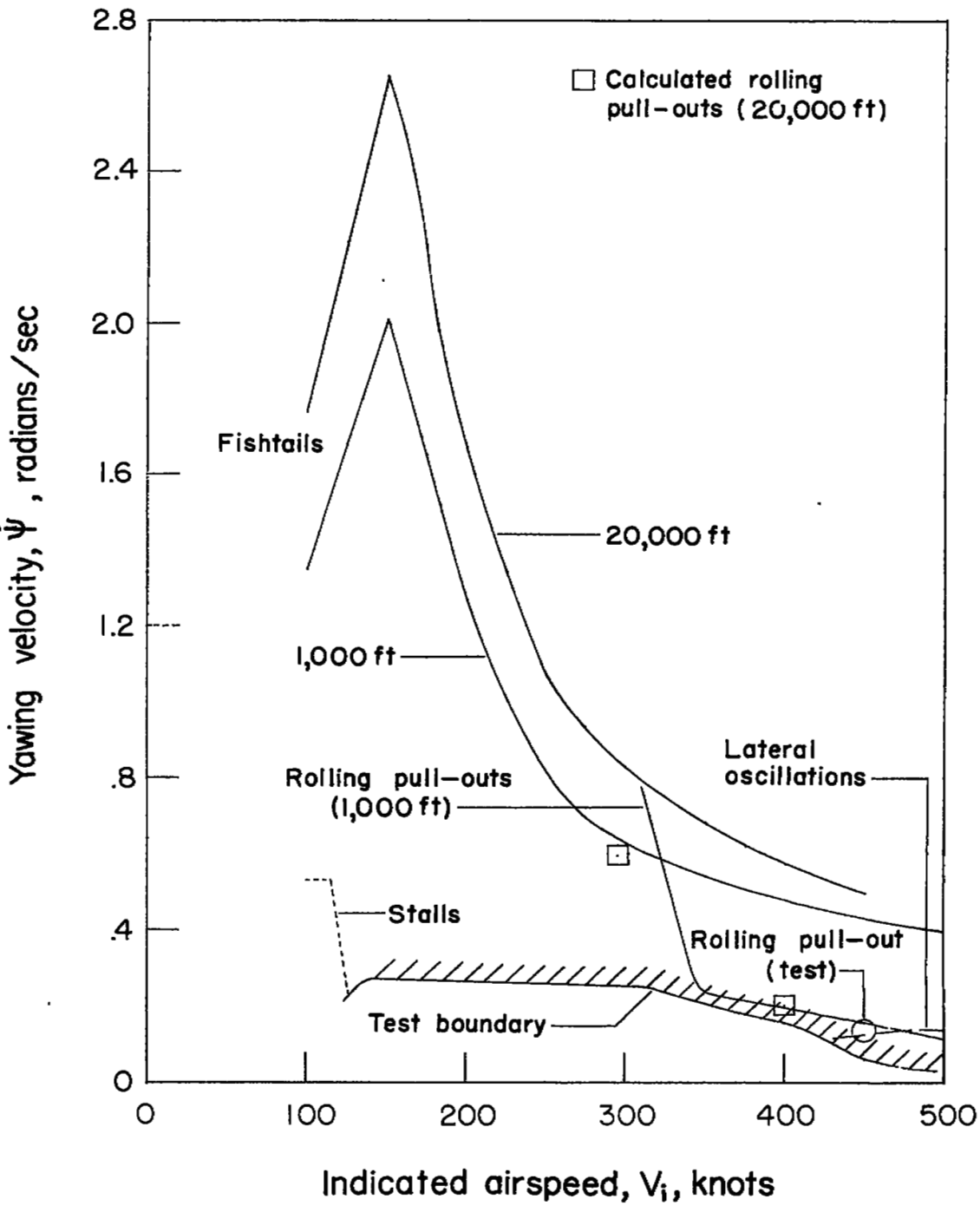

Figure 24.- Comparison of test results for the F-86A airplane with maximum calculated values of yawing velocity during fishtail and rolling pull-out maneuvers.

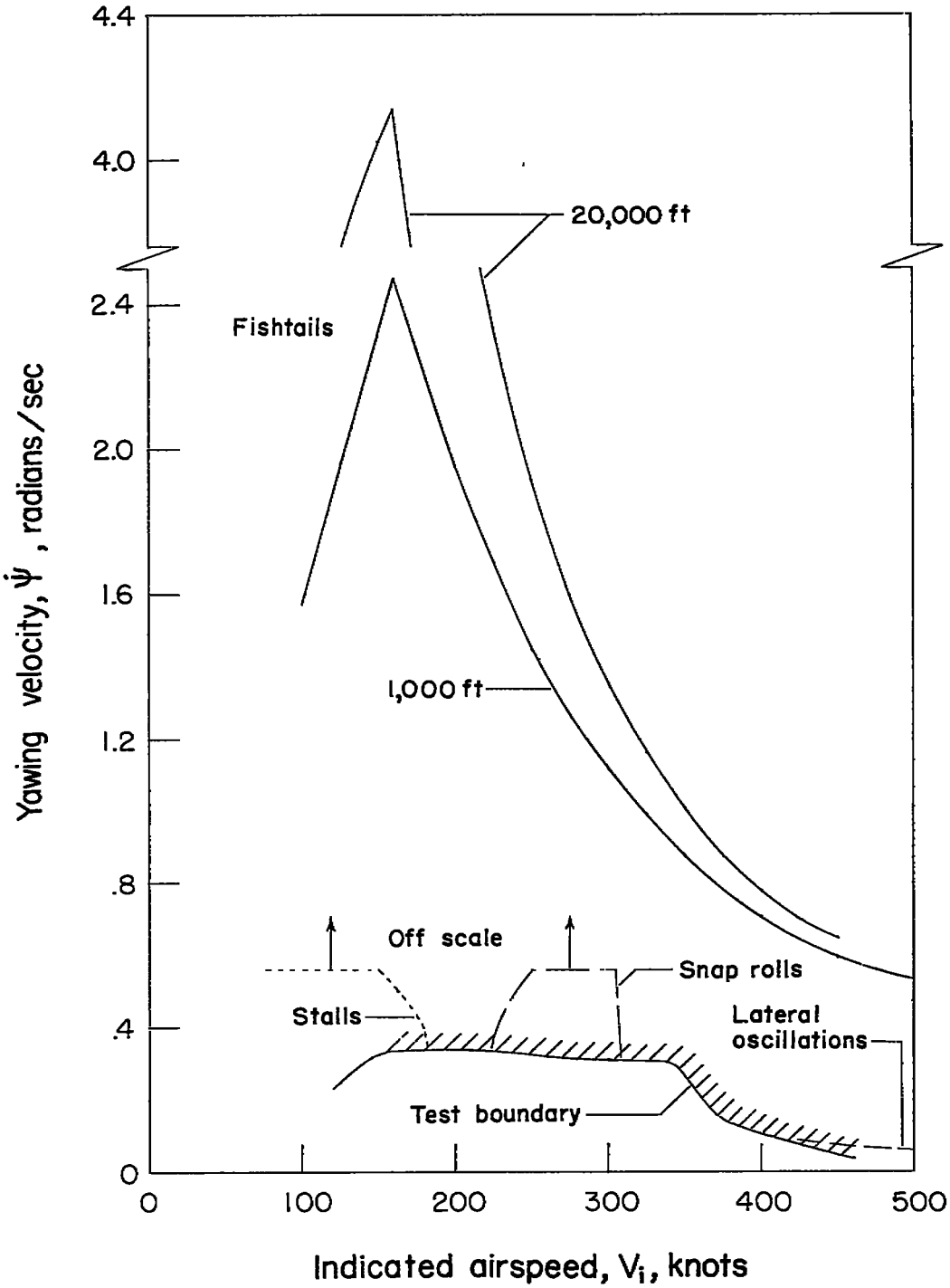

Figure 25.- Comparison of test results for the F-84 airplane with maximum calculated values of yawing velocity during fishtail maneuvers.

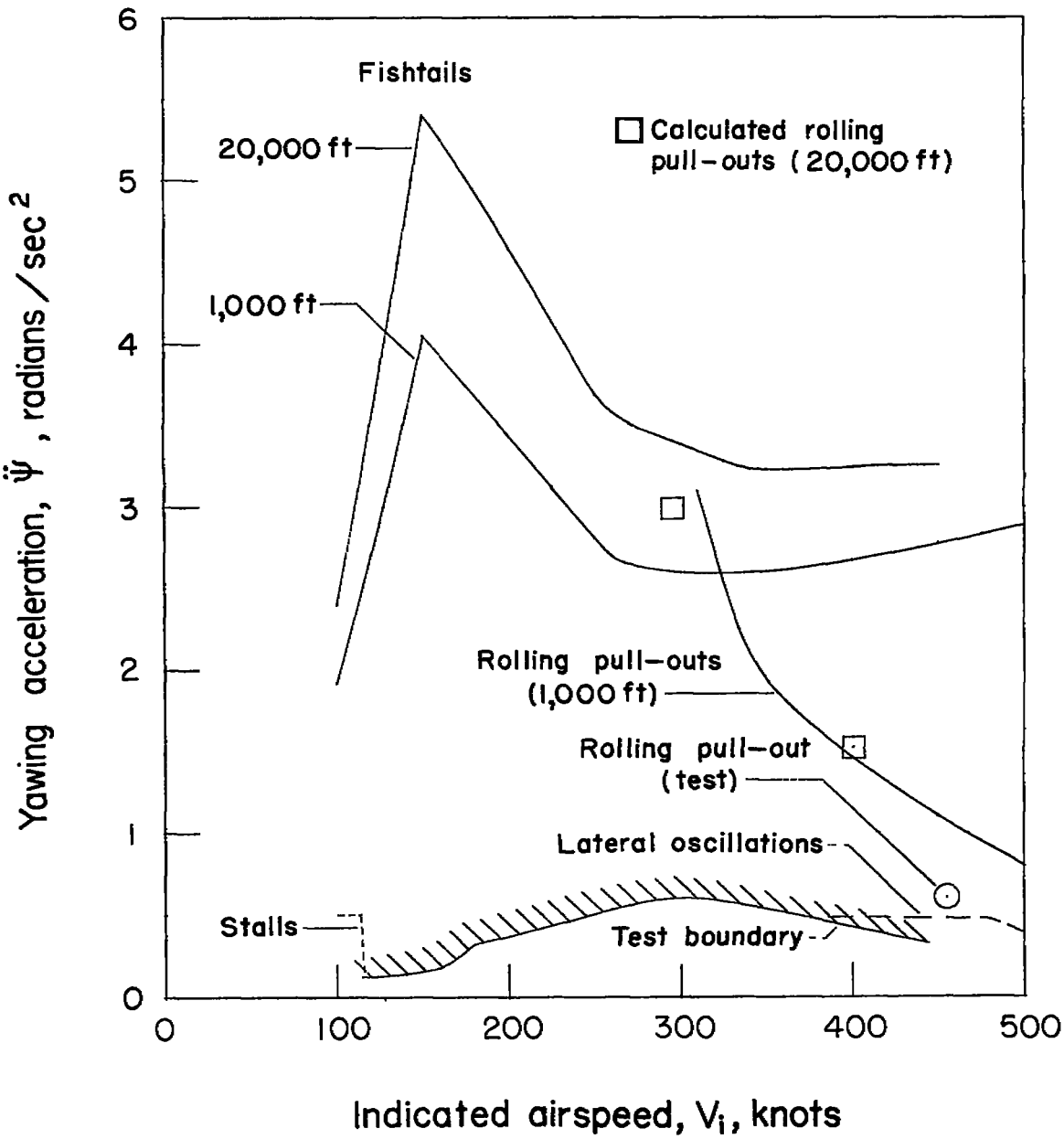

Figure 26.- Comparison of test results for the F-86A airplane with maximum calculated values of yawing acceleration during fishtail and rolling pull-out maneuvers.

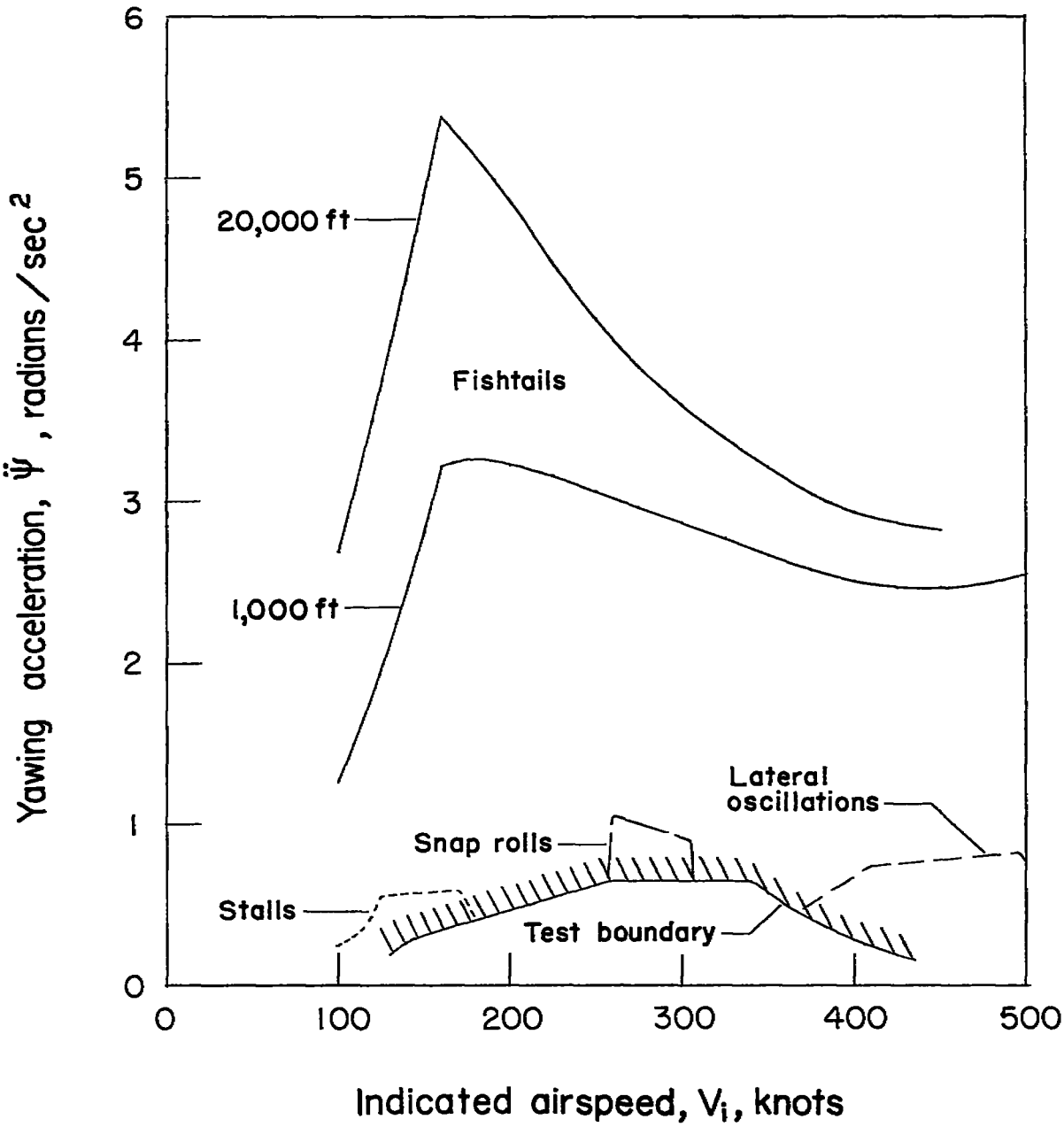

Figure 27.- Comparison of test results for the F-84 airplane with maximum calculated values of yawing acceleration during fishtail maneuvers.